Check for updates

Biotechnology and Bioengineering

WILEY

BIOTECHNOLOGY AND BIOENGINEERING

ARTICLE OPEN ACCESS

A General Workflow for Tangential Flow Filtration Perfusion Scale-Up

Patrick Romann[1] | Ken Lee[2] | Venkatesh Natarajan[3] | Daniel Ley[4] | Claes Nymand Nilsson[4] | David Garcia-Munzer[5] | Dominik Schieman[5] | Mahbod Hajighasemi[6] | Alex Zaytsev[7] | Jason Friedman[7] | Loic Chappuis[8] | Tobias Habicher[9] | Colin Jaques[10] | Alex Cohen[11] | Matthew Gagnon[12] | Edward Chan[13] | Daniel J. Karst[14] | Philip Giller[1] | Antony Sibilia[1] | Andrew L. Zydney[15] | Thomas K. Villiger[16]

[1]Levitronix GmbH, Zürich, Switzerland | [2]AstraZeneca, Gaithersburg, Maryland, USA | [3]Amgen, Cambridge, Massachusetts, USA | [4]Novo Nordisk, Hillerød, Denmark | [5]Novartis, Basel, Switzerland | [6]Merck & Co., Inc., Rahway, New Jersey, USA | [7]Just - Evotec Biologics, Seattle, Washington, USA | [8]Merck Serono, Corsier-sur, Vevey, Switzerland | [9]Boehringer Ingelheim Pharma GmbH & Co. KG, Biberach an der Riß, Germany | [10]Lonza, Slough, UK | [11]Eli Lilly, Indianapolis, Indiana, USA | [12]Pfizer, Andover, Massachusetts, USA | [13]Genentech, Oceanside, California, USA | [14]Biogen International GmbH, Luterbach, Switzerland | [15]The Pennsylvania State University, University Park, Pennsylvania, USA | [16]University of Applied Sciences and Arts Northwestern Switzerland, Muttenz, Switzerland

Correspondence: Thomas K. Villiger (thomas.villiger@fhnw.ch)

Received: 20 April 2026 | **Revised:** 20 April 2026 | **Accepted:** 29 July 2026

Keywords: cell retention device | hydraulic characterization | scale-down model | scale-up | TFF perfusion

ABSTRACT

Tangential flow filtration (TFF) perfusion using hollow-fiber modules offers substantial advantages over other mammalian cell retention technologies. Recently, increased awareness of Starling flow has helped to enhance filtration performance to similar, or even higher levels compared to alternative technologies. Despite these improvements, scaling TFF perfusion remains challenging and often requires time-consuming trial-and-error efforts. This manuscript presents a systematic, data-driven four-step workflow for designing and scaling TFF perfusion systems, integrating hydraulic considerations, bubble removal studies, and pump characterizations. While filter selection in TFF perfusion often receives significant attention, the design of the cell retention loop is commonly overlooked. However, this element plays a crucial role in system performance and can cause suboptimal pump operation, residence time issues, and bubble accumulation. The developed data-driven workflow facilitates the optimization of designs for generic TFF perfusion systems utilizing hollow-fiber modules, effectively bridging the gap between small-scale and manufacturing-scale implementations.

1 | Introduction

Perfusion cell cultures play a key role in current process intensification strategies, either by enhancing the productivity of existing fed-batch production facilities through N-1 perfusion or by serving as the main production bioreactor in continuous processes (Bielser et al. 2018; Wolf et al. 2020). Among the various cell retention technologies available, membrane systems composed of hollow fibers (HF) have emerged as the preferred choice in the industry (Pinto and Brower 2020; Matanguihan and Wu 2022; MacDonald 2022; Coffman 2021; Fisher et al. 2019). This preference is largely driven by their compatibility with single-use (SU) technologies, their ability to achieve complete cell retention through the size cutoff by the filter membrane, and their favorable scalability.

Abbreviations: ATF, alternating tangential flow filtration; CRD, cell retention device; FT, flow transmitter; HF, hollow fiber; HPTFF, high performance tangential flow filtration; ID, inner diameter; mAb, monoclonal antibody; OD, outer diameter; PES, polyether sulfone; PP, polypropylene; PS, polysulfone; PT, pressure transmitter; PVDF, polyvinylidene fluoride; rTFF, reverse tangential flow filtration; scTFF, stepping co-current tangential flow filtration; SU, single-use; TFF, tangential flow filtration; TMP, transmembrane pressure; TT, temperature transmitter; VCD, viable cell density; VCV, viable cell volume; VVD, vessel volume per day.

This is an open access article under the terms of the Creative Commons Attribution License, which permits use, distribution and reproduction in any medium, provided the original work is properly cited.

© 2026 The Author(s). *Biotechnology and Bioengineering* published by Wiley Periodicals LLC.

In general, two different systems operating in crossflow filtration mode (commonly known as tangential flow filtration, or TFF) are used in perfusion processes: One commonly used TFF perfusion setup is the single connection configuration, exemplified by the alternating tangential flow (ATF) operating mode (Figure 1A). This alternating flow pattern has shown benefits in lab- and pilot-scale studies, with improved product sieving, potentially due to the backflushing effect occurring on both sides of the HF module (Karst et al. 2016; Clincke et al. 2013; Wang et al. 2017). However, at manufacturing scale, air-operated diaphragm pumps have been associated with operational instability, unsteady crossflow behavior that complicates scalability, and leads to challenges at high cell densities due to elevated culture viscosity (Coffman 2021; Clincke et al. 2013; Shevitz 2018; Pavlik 2017a, 2019b; Walther et al. 2019; Clincke et al. 2011). While the plug-and-play nature of ATF systems is considered advantageous for accelerating development in early-phase clinical trials or commercial processes with low material requirements, their scalability is limited. In particular, the 1-pump-1-filter design and the limited volume of the diaphragm pump necessitates placing multiple HF modules in close proximity to the bioreactor to achieve the required filtration area, which results in substantial floor space demands at manufacturing scale, limitations in available bioreactor ports, and requires additional utilities in the facility such as vacuum and compressed air (Coffman 2021; Romann et al. 2023).

Another common configuration is the recirculating loop system, which is often simply referred to as tangential flow filtration (TFF) perfusion within the industry. These systems typically consist of a pump integrated into a tubing circuit that draws cell culture fluid from the bioreactor, passes it through a HF module at one end, and returns it to the bioreactor from the module exit (Figure 1B). This recirculating loop setup enables continuous, unidirectional crossflow through the HF module. The main pump types successfully applied to high density perfusion TFF reported in the literature are rotary lobe pumps (Amer et al. 2022; Johnstone et al. 2020), which are positive displacement pumps, and low-shear centrifugal pumps (Coffman 2021; Clincke et al. 2013), which belong to the class of dynamic pumps. Unlike positive displacement pumps, centrifugal pumps act as

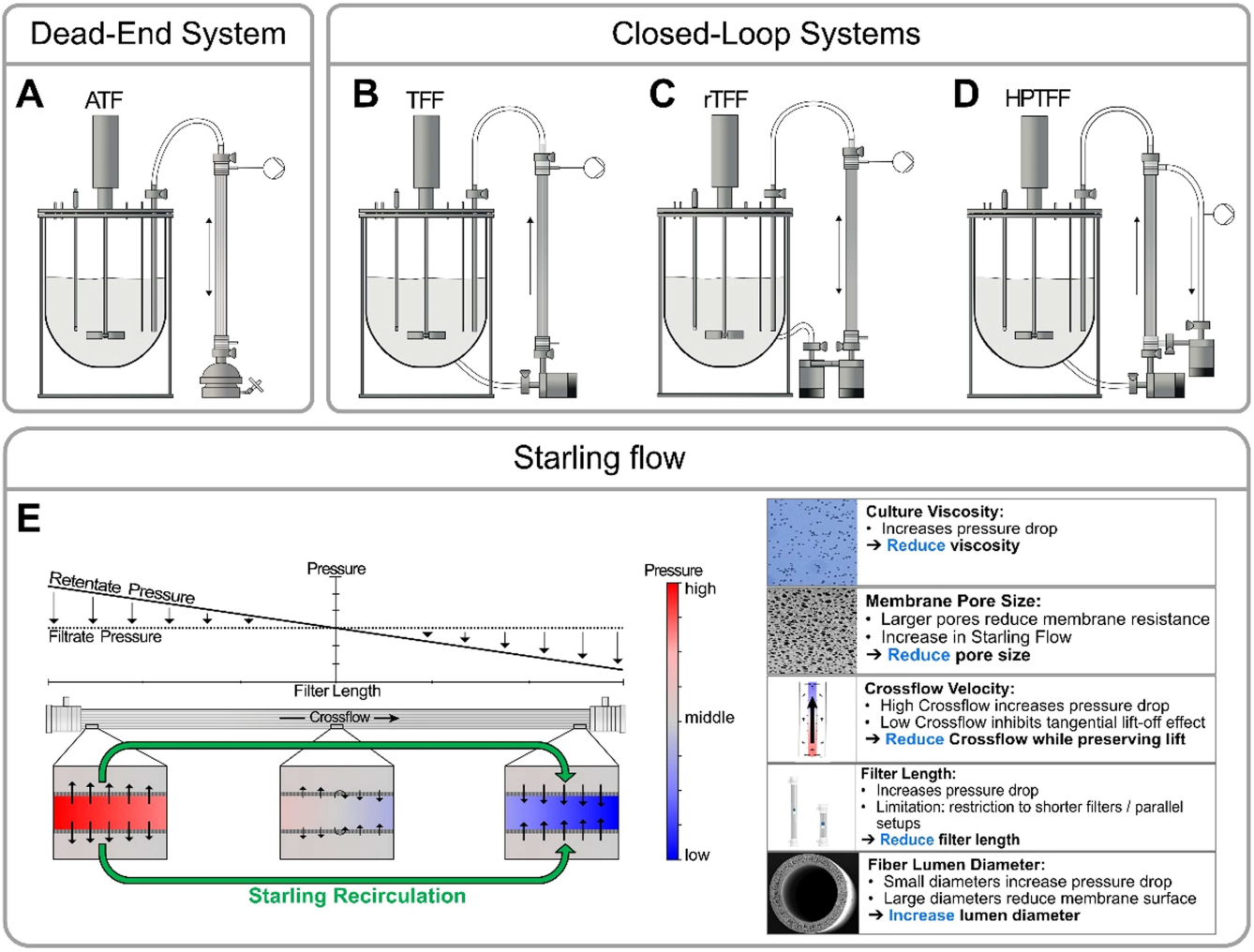

FIGURE 1 | Overview of various perfusion and filtration system configurations for benchtop bioreactors adapted from the literature (Romann et al. 2024). (A) Schematic of an ATF perfusion system with a diaphragm pump and filter, representing a "dead-end system", (B) a simple TFF system with one pump and unidirectional flow through the filter, (C) an rTFF system with two pumps enabling an alternating flow, and (D) a HPTFF setup with two pumps, one on the feed and one on the filtrate recirculation loop, enabling a uniform pressure distribution across the membrane. (E) Diagram illustrating Starling flow within a hollow fiber filter, accompanied by strategies to mitigate its effects.

10970290, 0, Downloaded from https://analyticalsciencejournals.onlinelibrary.wiley.com/doi/10.1002/bit.70335 by Fachhochschule Nordwestschweiz, Wiley Online Library on [28/08/2026]. See the Terms and Conditions (https://onlinelibrary.wiley.com/terms-and-conditions) on Wiley Online Library for rules of use; OA articles are governed by the applicable Creative Commons License

pressure sources rather than flow sources, and their operating speed is therefore strongly influenced by the hydraulic design of the flow path. Nevertheless, suboptimal flow path design and the resulting elevated hydraulic load have also been identified as critical challenges for rotary lobe pumps. High backflows within the pump head can generate excessive shear, making hydraulic system design a pump-independent critical design parameter (Amer et al. 2022). Most TFF skids are currently customized and thus flow path design may cause challenges at larger scales. For N-1 perfusion in the multi-thousand liter scale, several unidirectional TFF setups have been successfully implemented using several pump technologies (Coffman 2021; Stepper et al. 2020). For N-stage perfusion, several literature reports have indicated a faster sieving decay in unidirectional TFF systems compared to alternating flow systems when operated at similarly high crossflow rates as a result of suboptimal custom design and operation (Karst et al. 2016; Pappenreiter et al. 2023; Romann et al. 2024).

Despite some reported limitations in filtration performance, there is a clear trend in the industry toward the adoption of systems operating in TFF mode largely due to their operational advantages, especially when perfusion processes are envisioned at high cell densities and scales larger than 500 liters (Coffman 2021). This trend has triggered extensive research aimed at closing the performance gap between ATF and TFF systems with the following main findings:

i. **Reduction of starling flow in unidirectional TFF systems:** The main benefit of operating in unidirectional TFF mode lies in the simplicity and low complexity, both in terms of technical and mechanical design, as well as in control system implementation. While alternating systems benefit from Starling flow due to the backflushing effect at both ends of the filter, that helps remove the accumulated material from within the concentration boundary layer (Raza et al. 2024; Veje et al. 2024), unidirectional TFF systems do not experience this benefit given that the Starling flow remains unidirectional (Starling 1896). Therefore, minimizing Starling flow is essential to avoid excessive and unnecessary filtration flux. This reduction, often resulting in wall shear rates below 1000 s^{-1}, can be achieved by lowering the pressure drop within the hollow fiber lumen (Raza et al. 2024; Lee 2022; WuDunn et al. 2024; Vu et al. 2024). Additional strategies to reduce Starling flow include increasing the lumen inner diameter of the HF module, shortening the filter length, or increasing membrane resistance (Romann et al. 2024; Lee 2022; WuDunn et al. 2024; Vu et al. 2024; Radoniqi et al. 2018) (Figure 1E).

ii. **Reversing crossflow in TFF systems:** By upgrading unidirectional TFF systems with a second, inversely oriented pump, alternating flow can be introduced, a configuration referred to as reverse TFF (rTFF) (Figure 1C). Despite higher complexity given an additional pump and control strategy, this setup allows for significant improvements in sieving performance while preserving most core advantages of unidirectional TFF systems (Pappenreiter et al. 2023; Romann et al. 2024; Weinberger et al. 2023; Sibilia 2022). Unlike ATF systems where cycle times are constrained by diaphragm pump volume and typically limited to a few seconds, rTFF systems offer far greater flexibility. Cycle times ranging from seconds to several hours can be implemented, opening new opportunities for optimizing process performance. This approach is particularly beneficial for processes involving large cell aggregates, which are prone to blocking hollow fiber inlets.

iii. **Elimination of starling flow by co-current filtrate flow:** Another alternative filtration method introduces a co-current filtrate flow along the membrane, outside the hollow fibers, thereby eliminating Starling flow in unidirectional TFF systems (van Reis et al. 1997). This approach, referred to as high-performance TFF (HPTFF) (Figure 1D), has demonstrated significant improvements in product sieving (Romann et al. 2024; Lee 2022). However, increased system complexity requires a more sophisticated control strategy and design changes to existing HF modules would be required to ensure scalability.

While the industry has found effective ways to address performance-related shortcomings, an increasing number of TFF perfusion processes are now progressing to commercial scale. The current major challenge lies in translating performance improvements, mostly developed at small to pilot scale, into reliable, scalable solutions for manufacturing. Regardless of which TFF perfusion mode is chosen for a given process (unidirectional TFF, rTFF, or HPTFF), all configurations share a common recirculating cell circuit composed of tubing, connectors, pump(s), and one or more HF modules (Figure 1B–D).

Notably, the filtration performance is often limited by process-specific fouling—driven by the accumulation of a "gel layer" composed of genomic DNA, cell debris, and hydrophobic antifoam (Madabhushi et al. 2025). As a consequence, the HF filter is often viewed as the most critical component of the cell retention loop whilst the design of the hydraulic loop has emerged as a blind-spot in the implementation of TFF perfusion systems (Johnstone et al. 2020; Schaub 2024). Whereas process-specific fouling is highly dependent on proprietary processes, hydrodynamic conditions can be compared across processes and scales and yet are still too frequently approached through trial and error, an approach that is both costly and time-consuming.

Therefore, the scope of this work is to summarize the current industry understanding of the most critical parameters for scaling TFF perfusion systems and to propose a general workflow that enables the transition from empirical, trial-and-error scaling to a faster, more reliable, calculation-based and data-driven approach. While broadly applicable to various pump technologies, this workflow is demonstrated using practical guidelines and data from levitated centrifugal pumps due to their industry-wide adoption.

2 | Materials and Methods

2.1 | Critical Flow Velocity Characterization

To determine the critical flow velocity in tubing of various inner diameters, two water-based test setups were used (Supporting

10970290, 0, Downloaded from https://analyticalsciencejournals.onlinelibrary.wiley.com/doi/10.1002/bit.70335 by Fachhochschule Nordwestschweiz, Wiley Online Library on [28/08/2026]. See the Terms and Conditions (https://onlinelibrary.wiley.com/terms-and-conditions) on Wiley Online Library for rules of use; OA articles are governed by the applicable Creative Commons License

Information S1: Figure S1). The method involved injecting air bubbles into a flowing liquid stream and identifying the lowest flow velocity at which bubbles remained in motion, defined as the critical flow velocity.

For smaller tube sizes, a 2-liter glass bottle with bottom outlet (Schott AG) equipped with a heating mantle served as the water reservoir. The temperature was maintained at 37°C using a heating and cooling thermostat (LAUDA Alpha RA, Lauda Scientific) and monitored with a PT100 probe (PendoTECH TT1, Pendotech). A circulation loop was built, incorporating a levitated centrifugal pump (PuraLev i30-SU, Levitronix GmbH), a clamp-on flow sensor (LFSC-i13X.1, Levitronix GmbH) with a LEVIFLOW® single-use flow pipe (LFP-13SU, Levitronix GmbH), and a Luer-Lock port with inner diameter of 2.5 mm in the vertical section of the tubing for injecting macro air bubbles. Silicone tubing with inner diameters of 1/8" (3.175 mm), 1/4" (6.35 mm), and 3/8" (9.525 mm) was tested. For larger tube sizes, a 115-liter stainless steel tank was used as the reservoir. The tank was heated to 37°C via a coil connected to a thermostat (LAUDA Alpha RA, Lauda Scientific), with temperature monitored using a PT100 probe. The loop included a levitated centrifugal pump (PuraLev DCP-2000.1, Levitronix GmbH), a clamp-on flow sensor (LFSC-i36X.1, Levitronix GmbH) with a LEVIFLOW single-use flow pipe (LFP-36SU.1, Levitronix GmbH), and a Luer-Lock port for bubble injection. Tubing with inner diameters of 1/2" (12.7 mm), 3/4" (19.05 mm), 1" (25.4 mm), 1 3/8" (34.925 mm), and 2" (50.8 mm) was tested.

After priming the loop, the flow rate was adjusted to a defined starting velocity. Air bubbles were introduced into the system using a 50 mL syringe (Corning Inc.) through the Luer-Lock port. Tubing was held against a dark background to visualize bubble movement. Flow was gradually reduced until a bubble remained stationary in the vertical portion of the flow path where the buoyant force opposes the direction of flow, indicating the critical velocity (Equation (6)). Measurements were conducted at fluid viscosities of 0.7 cP (water at 37°C), 2.5 cP, and 5 cP, the latter two achieved by mixing water and glycerin (99.5%, REF: BE-13023), adjusted using a viscometer (Viscometer Head VMH-30SU.1, Levitronix GmbH).

2.2 | Pump Characterization

A water-based test setup was used to characterize the levitated centrifugal pump family (PuraLev, Levitronix GmbH) under minimal hydraulic system load (SI Figure 2). Separate loops were designed for small-scale and large-scale pumps to generate accurate pressure and flow data across scales. For the small-scale setup, pressure was measured using transmitters PT1 and PT2 (PREPS-N-038, PendoTECH), while flow was monitored using a flow transmitter FT1 (LFSC-i10X, Levitronix GmbH). The temperature inside the tank and loop was controlled at 37°C using a heating stirring plate (Roth, ROTILABO MH 20) and monitored with an integrated temperature transmitter TT1. A manual valve (DN10, Flowtech Inc.) was used to control system backpressure. The valve was gradually adjusted to regulate flow resistance during the experiment. A similar experimental setup for pressure characterization was built for large-scale experiments to achieve accurate system characterizations. The pressures in the setup were measured using pressure transmitters PT1 and PT2 (PREPS-N-5-5, PREPS-N-1-1, PREPS-N-15-15, PendoTECH), and the flow was measured using flow transmitter FT1 (OPTIFLUX 7300 FL, KROHNE Group). A ball valve (DN80, SUNTHAI) was installed to control the back-pressure. The pump head characteristics for both the small-scale (Supporting Information S1: Table S1) and large-scale loops (Supporting Information S1: Table S2), including the tubing and sensor IDs, are detailed in the supporting information section. Pump impeller tip speed was initially set to 1 m/s with the valve fully open. The valve was then gradually closed in steps while maintaining a constant rpm. This procedure was repeated, increasing the tip speed in 0.5 m/s increments up to a maximum of 10 m/s. Differential pressure across the pump was calculated using the following equation:

$$\Delta \mathbf{P}_{\boldsymbol{Pump}} = \boldsymbol{PT_2} - \boldsymbol{PT_1} \tag{1}$$

The calculated pump differential pressures (ΔP_{Pump}) were subsequently plotted against the corresponding flow rates, resulting in the pressure-flow characterization.

2.3 | Relevant Equations for the TFF Perfusion Scaling Workflow

2.3.1 | VCV Calculation From VCD Cell Count

The viable cell volume fraction (VCV) was calculated based on the assumption of a spherical cell shape using Equation (2) (Metze et al. 2020):

$$\mathbf{VCV} = \frac{\mathbf{4}}{\mathbf{3}} \cdot \boldsymbol{\pi} \cdot \left(\frac{\boldsymbol{D_{cell}}}{\mathbf{2}}\right)^{\mathbf{3}} \cdot \boldsymbol{VCD} \cdot \mathbf{100} \tag{2}$$

where D_{cell} is the average cell diameter [μm] and VCD is the viable cell density [10^6 cells/mL]. The resulting VCV is expressed as a percentage of the total culture volume.

2.3.2 | Fluid Stream Calculation for Perfusion Processes

For continuous perfusion processes, the volumetric harvest flow rate was calculated as the difference between the perfusion and bleed flow rates:

$$\boldsymbol{Q_{Harvest}} = \boldsymbol{Q_{Perfusion}} - \boldsymbol{Q_{Bleed}} \tag{3}$$

where $Q_{Harvest}$, $Q_{Perfusion}$, and Q_{Bleed} are the volumetric harvest, perfusion, and bleed flow rates [L/day].

The normalized perfusion rate P, expressed in vessel volumes per day [vvd], was determined according to:

$$\boldsymbol{P} = \frac{\boldsymbol{Q_{Perfusion}}}{\boldsymbol{V_R}} \tag{4}$$

where $Q_{Perfusion}$is the volumetric perfusion flow rate [L/day] and V_R denotes the bioreactor working volume [L].

The normalized permeate flux (LMH) was calculated as follows:

10970290, 0, Downloaded from https://analyticalsciencejournals.onlinelibrary.wiley.com/doi/10.1002/bit.70335 by Fachhochschule Nordwestschweiz, Wiley Online Library on [28/08/2026]. See the Terms and Conditions (https://onlinelibrary.wiley.com/terms-and-conditions) on Wiley Online Library for rules of use; OA articles are governed by the applicable Creative Commons License

$$J_{Filtrate} = \frac{Q_{Harvest}}{A_{Filter} \cdot 24} \quad (5)$$

where $J_{Filtrate}$ is the flux, expressed in liters per square meter per hour [L/m^2/h], and commonly referred to as LMH in the industry, $Q_{Harvest}$ is the harvest flow rate [L/day], and A_{Filter} is the membrane surface area [m^2].

2.3.3 | Flow Velocity, Shear Rate and Shear Stress Calculations

To assess hydrodynamic conditions in tubing systems, the linear flow velocity ϑ was determined from the volumetric flow rate and tube geometry:

$$\vartheta = \frac{Q}{\pi \cdot r^2 \cdot 60000} \quad (6)$$

where ϑ is the linear flow velocity [m/s], Q is the volumetric fluid flow rate [L/min], and r is the tube radius [m].

The wall shear rate for laminar flow in a circular tube was calculated using Equation (7):

$$\dot{\gamma} = \frac{4 \cdot Q}{\pi \cdot r^3 \cdot 60000} \quad (7)$$

where $\dot{\gamma}$ is the shear rate [1/s], Q is the volumetric fluid flow rate [L/min], and r is the tube radius [m].

The shear rate between two moving parallel walls was calculated using Equation (8):

$$\dot{\gamma} = \frac{\vartheta}{D} \quad (8)$$

where $\dot{\gamma}$ is the shear rate [1/s], ϑ is the linear flow velocity [m/s], and D is the distance between the walls [m].

Shear stress τ was calculated by multiplying the viscosity μ of the fluid with the shear rate $\dot{\gamma}$:

$$\tau = \mu \cdot \dot{\gamma} \quad (9)$$

where τ is the shear stress [Pa], μ is the fluid viscosity [Pa·s], and $\dot{\gamma}$ is the shear rate [1/s].

2.3.4 | Hydraulic System Load Calculation

The pressure drop in a tube (or fiber lumen) was calculated using the Darcy-Weisbach equation:

$$\Delta P = \frac{8 \cdot \rho \cdot f}{\pi^2} \cdot \frac{L \cdot (Q/60000)^2}{D^5} \quad (10)$$

where ΔP is the pressure drop [Pa], ρ is the fluid density [kg/m^3], f is the Darcy friction factor, L is the tube or fiber lumen length [m], Q is the volumetric fluid flow rate [L/min], and D is the tube or lumen inner diameter [m].

For laminar flow, the friction factor f was calculated using Equation (11), assuming a Reynolds number below 2200 to define laminar flow (Reynolds 1883):

$$f = \frac{64}{Re} \quad (11)$$

The Reynolds number Re was calculated as:

$$Re = \frac{\rho \cdot \vartheta \cdot D}{\mu} \quad (12)$$

where ρ is the fluid density [kg/m^3], ϑ is the linear flow velocity [m/s], D is the inner diameter of the tube or lumen [m], and μ is the dynamic viscosity of the fluid [Pa·s].

To estimate the friction factor in turbulent flow regimes, the Haaland equation was used:

$$\frac{1}{\sqrt{f}} = -1.8 \cdot \left[\left(\frac{\varepsilon/D}{3.7} \right)^{1.11} + \frac{6.9}{Re} \right] \quad (13)$$

where ε is the absolute roughness of the tube or lumen [m], ε/D is the relative roughness. A conservative absolute roughness for the HF lumen of 0.1 mm was assumed and 0.01 mm for silicone tubing (Merivirta 2017).

The overall hydraulic system load of the cell retention system can be calculated by summing the individual hydraulic pressure drop contributions from each system component, as shown below:

$$\Delta P_{overall} = \Delta P_{HF} + \Delta P_{Tubing} + \Delta P_{Connectors} + \Delta P_{Pump} \quad (14)$$

Where $\Delta P_{overall}$ is the overall hydraulic system load, ΔP_{HF} the hydraulic contribution of the HF module, ΔP_{Tubing} the hydraulic contribution of the tubing, $\Delta P_{Connectors}$ the hydraulic contribution of the connectors and ΔP_{Pump} the hydraulic contribution of the pump.

2.3.5 | Residence Time Calculation in Loop

The average residence time of fluid circulating through the cell retention loop (including filter, tubing and pump) was calculated using Equation (15):

$$t_{Loop} = \frac{(V_{Filter} + V_{Tube} + V_{Pump}) \cdot 60}{Q} \quad (15)$$

where t_{Loop} is the average residence time [s], V_{Filter}, V_{Tube}, and V_{Pump} are the respective component volumes [L], and Q is the fluid flow rate [L/min]. V_{Pump} values can be found in SI Table 3.

2.3.6 | Pump-Related Equations

The tip speed of the pump impeller was calculated using Equation (16):

10970290, 0, Downloaded from https://analyticalsciencejournals.onlinelibrary.wiley.com/doi/10.1002/bit.70335 by Fachhochschule Nordwestschweiz, Wiley Online Library on [28/08/2026]. See the Terms and Conditions (https://onlinelibrary.wiley.com/terms-and-conditions) on Wiley Online Library for rules of use; OA articles are governed by the applicable Creative Commons License

$$v_{tip} = \frac{\pi \cdot D_{impeller} \cdot n}{60} \quad (16)$$

where v_{tip} is the tip speed [m/s], $D_{impeller}$ is the impeller diameter [m], and n is the rotational speed in revolutions per minute (rpm). $D_{impeller}$ values can be found in SI Table 3.

To quantify the number of reactor turnovers per day via recirculating pumps, the turnover rate was calculated as:

$$T_d = \frac{N_{cluster} \cdot Q_{cluster} \cdot 1440}{V_R} \quad (17)$$

where T_d is the turnover rate [1/day], $N_{cluster}$ is the number of clusters present on the bioreactor, $Q_{cluster}$is the cluster fluid flow rate [L/min], and V_R is the bioreactor fill volume [L]. A cluster refers to the defined assembly of pumps, tubing, and filtration modules that constitute the recirculating cell retention loop, with multiple clusters often employed at larger scales to enhance throughput and process robustness.

The average residence time of fluid in the pump head per turnover was calculated using Equation (18):

$$t_{Pump} = \frac{V_{Pump} \cdot 60}{Q_{cluster}} \quad (18)$$

where t_{Pump} is the residence time in the pump head [s], $Q_{cluster}$is the cluster fluid flow rate [L/min], and V_{Pump} is the pump head volume [L].

3 | Results and Discussion

Designing an effective TFF cell retention solution can be divided into two distinct phases. In the first phase, process-specific design inputs are defined to ensure proper alignment between the equipment and the intended perfusion process. These inputs vary significantly across the industry, depending on the cell line, product, and operational strategy. In the second, process-independent phase, scale-relevant design inputs are incorporated to ensure that the TFF cell retention system is properly dimensioned for reliable operation under the defined process-specific conditions. Given the high variability in process-specific requirements and the wealth of literature already available on this topic, this manuscript provides only a brief overview of key parameters and typical industry ranges that may serve as a starting point for evaluation. The primary focus of this work is to present a clear, structured workflow for addressing the scaling challenges of TFF cell retention systems, one that can be applied regardless of the specific process context. An overview of the proposed TFF perfusion scaling workflow is provided in Figure 2.

3.1 | Process-Specific Design Inputs for TFF Systems

Process-specific design inputs for TFF cell retention systems can be broadly categorized into the following groups: cell culture parameters, fluid handling parameters, and filter-related parameters, including both filter characteristics and operating conditions. These inputs are essential to ensure compatibility between the process and the equipment setup, supporting

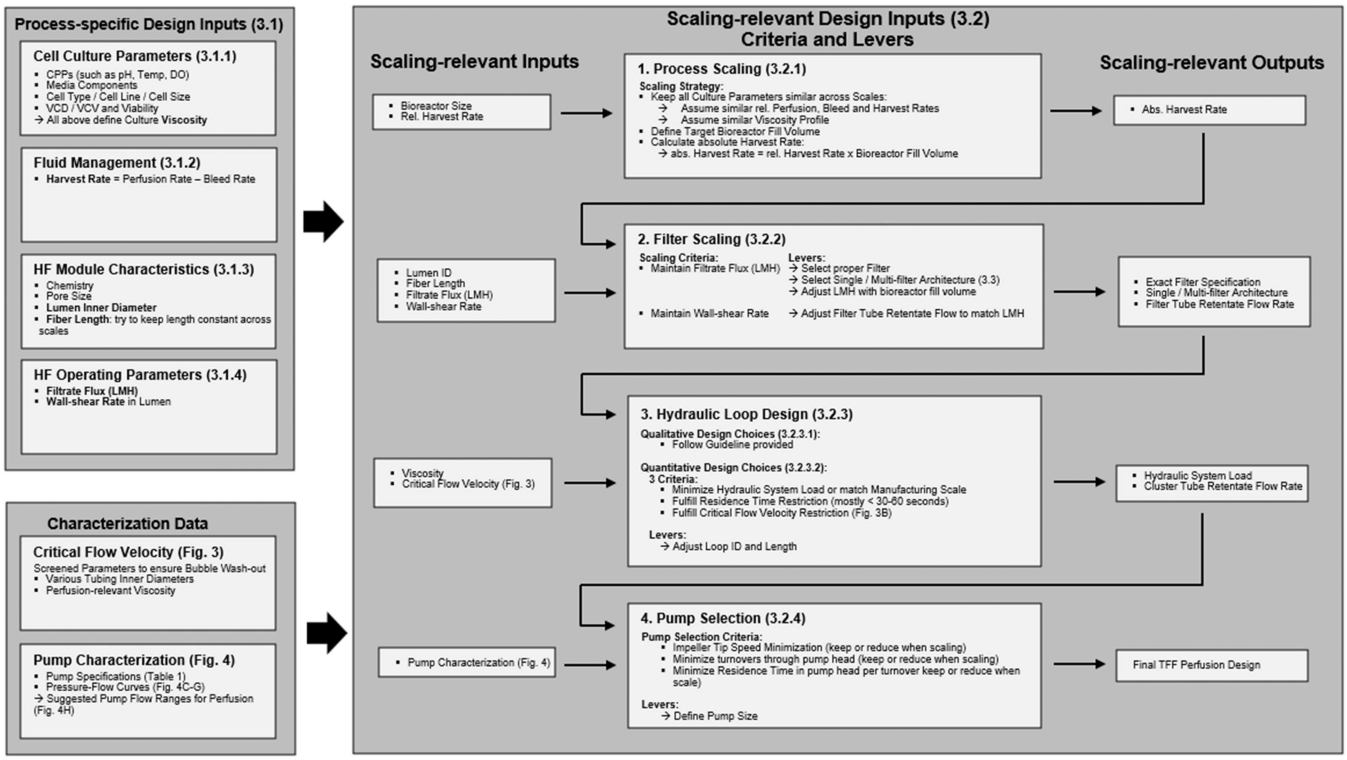

FIGURE 2 | Overview schematic of proposed TFF perfusion scaling workflow. Process-specific design inputs as well as characterization data provided in this manuscript feed into the proposed 4-step TFF scaling approach. The scaling approach consists of the following 4 steps: 1. Process Scaling; 2. Filter Scaling; 3. Hydraulic Loop Design; 4. Pump Selection.

10970290, 0, Downloaded from https://analyticalsciencejournals.onlinelibrary.wiley.com/doi/10.1002/bit.70335 by Fachhochschule Nordwestschweiz, Wiley Online Library on [28/08/2026]. See the Terms and Conditions (https://onlinelibrary.wiley.com/terms-and-conditions) on Wiley Online Library for rules of use; OA articles are governed by the applicable Creative Commons License

robust execution of process control strategies. Typical ranges for these parameters observed across the industry are summarized below, providing a useful reference point for initial system sizing and evaluation.

3.1.1 | *Cell Culture Parameters*

Cell densities of 50 to 100 million cells/mL are common in modern perfusion processes, with some reports indicating densities as high as 200 million cells/mL (Clincke et al. 2011; Zamani 2018). While viable cell density (VCD) is a well-established metric, viable cell volume fraction (VCV) which is representing the biomass more appropriately (Equation (2)), may offer a more meaningful basis for comparing perfusion processes (Metze et al. 2020). Common VCV values reach up to 30%, with recent efforts pushing this even higher (Romann et al. 2023; Caso et al. 2022). In addition to VCD and VCV, viscosity of the cell culture is an important design consideration. Viscosity reflects both cell concentration and changes in cell viability. For most perfusion processes, viscosity remains in the range of 1 to 2 cP but can rise up to 5 cP in high-viability cultures (Clincke et al. 2013; Tregidgo et al. 2023). Lower cell viability at later stages of the cell culture can result in an additional sharp increase in viscosity, often exceeding 5 cP as per authors' experience.

3.1.2 | *Fluid Management*

The harvest rate of a perfusion process is a key input for properly sizing the cell retention system, as it directly affects the flux through the filter (Equation (3)). Most steady-state perfusion processes operate at perfusion rates between 1 and 2 vessel volumes per day (vvd) (Equation (4)), with bleed rates typically ranging from 10 to 20 percent of the perfusion rate. As a result, the harvest rate generally accounts for 80 to 90 percent of the perfusion rate (Bielser et al. 2018). In dynamic perfusion processes, the harvest rate is equal to the perfusion rate.

3.1.3 | *HF Module Characteristics*

Hollow fiber membranes used in perfusion cell culture applications are primarily made from polyether sulfone (PES), polysulfone (PS), or polyvinylidene fluoride (PVDF) (Raza et al. 2024). One of the design parameters is the inner diameter of the fiber lumen, which influences both hydraulic performance and filtration behavior. A larger lumen inner diameter generally reduces the pressure drop along the fiber, resulting in lower Starling flow and lower required pump speeds due to decreased hydraulic resistance. However, increasing the lumen diameter also reduces the available membrane surface area, as fewer fibers can be packed into a given filter housing owing to the reduced surface area to volume ratio. Lumen diameters between 1.0 and 1.4 mm are most commonly used for perfusion applications in the industry. Filter length is another parameter that affects hydraulic pressure drop. Longer filters increase the pressure drop across the membrane, which in turn leads to higher Starling flow (Lee 2022; Vu et al. 2024). A length between 60 and 100 cm is commonly selected, even though shorter modules between 20 and 40 cm are often utilized in bench scale and automated reactor systems. Although larger pore sizes have been explored to increase membrane flux and reduce product retention, a pore size of 0.2 μM is the standard for most perfusion processes (Coffman 2021). This allows the harvested material to be sent directly to downstream processing without additional filtration steps. In processes where the product is retained in the bioreactor, such as monoclonal antibody production, smaller pore sizes with a molecular weight cutoff less than 50 kDa are typically used.

3.1.4 | *HF Operating Parameters*

Membrane fluxes in TFF perfusion systems are typically expressed in $L/m^2/h$ (commonly referred to as LMH), which normalizes the flow rate by the membrane surface area (Equation (5)). For N-stage perfusion processes where product sieving is critical, lower LMH values between 2 and 6 LMH are commonly used (Raza et al. 2024; Recanati 2023). In contrast, higher LMH values, up to 20, are often applied in N-1 perfusion processes where product retention is not a concern (Kudugunti 2022). Another key parameter is the effective crossflow, which directly impacts the sizing of tubing and components in the cell retention loop. Crossflow is defined by the target wall shear rate inside the hollow fiber lumen (Equation (7)). While earlier studies operated systems at shear rates of 1500–2000 s^{-1} or higher, current TFF perfusion processes typically use lower shear rates in the range of 400–1000 s^{-1} (Raza et al. 2024; Lee 2022; WuDunn et al. 2024; Vu et al. 2024). This shift is driven by improved filtration performance at lower shear conditions, as well as the desire to reduce shear stress on the cell culture.

3.2 | Scale-Relevant Design Inputs for TFF Systems

Once reasonable process-specific design inputs have been defined, either based on prior process knowledge or through dedicated development work, the next critical challenge is to scale the TFF cell retention system in a way that maintains process performance across different scales. To address this, the authors developed a systematic workflow grounded in current industry practices and supported by novel characterization data. This workflow is intended to guide users through the key steps required for reliable and predictable scale-up. It consists of four main stages: 1. Process scaling, 2. Filter scaling, 3. Hydraulic loop design, 4. Pump selection (Figure 2).

3.2.1 | *Process Scaling*

When scaling up a TFF perfusion process, key process inputs or outputs such as cell concentration profiles, expressed as either VCD or VCV, and the relative perfusion rate profile in vvd, are typically maintained across scales. It is further assumed that the cell viability profiles, and therefore culture viscosity profiles remain comparable across scales. Assuming a comparable bleed fraction profile, if applicable, and a robust process with scale-independent cell doubling times, the absolute harvest rate increases linearly with bioreactor scale.

3.2.2 | *Filter Scaling*

The rationale behind filter selection is to maintain consistent filter characteristics to preserve filtration performance across scales. This is relatively straightforward for parameters such as

10970290, 0, Downloaded from https://analyticalsciencejournals.onlinelibrary.wiley.com/doi/10.1002/bit.70335 by Fachhochschule Nordwestschweiz, Wiley Online Library on [28/08/2026]. See the Terms and Conditions (https://onlinelibrary.wiley.com/terms-and-conditions) on Wiley Online Library for rules of use; OA articles are governed by the applicable Creative Commons License

membrane chemistry, lumen inner diameter, and pore size, as most filter manufacturers offer a range of filter sizes while keeping these characteristics constant.

The main operational filter scaling criterion used in the industry is to keep the normalized filtrate flux, measured in LMH, constant across scales (Equation (5)). As the required absolute harvest rate increases with scale, a larger filtration area is needed to achieve the same LMH. Changing the filter length during scale-up to increase filtration area alters the amount of Starling flow, which can unpredictably impact filtration performance. Therefore, a unified HF module length across all scales is strongly preferred for scale-down models assessing cell retention device performance, to ensure consistent and predictable performance (Romann et al. 2024). In addition to filter length, this manuscript recommends keeping the wall shear rate within the HF lumen constant across scales (Equation (7)). Together with consistent filter length, this ensures that the flow conditions within each individual fiber remain similar, supporting consistent performance across different scales. It is important to note that the influence on Starling flow becomes less pronounced when using HF modules with a larger lumen inner diameter. Filtrate flux can further be fine-tuned by slightly adjusting the bioreactor fill volume or by introducing a recycle loop that returns a portion of the permeate back to the bioreactor, which artificially increases LMH at benchtop scales. In practice, the filter length is typically maintained constant during scale-up whenever possible. At smaller scales, such as the AMBR 250 mL perfusion system, maintaining manufacturing filter length may be impractical or unfeasible. Conversely, at larger scales, limiting the filter length could restrict the available filter area, leading to excessively wide filters.

3.2.3 | *Hydraulic Loop Design*

The hydraulic loop of a TFF perfusion system includes all components that come into contact with the cell culture fluid. This encompasses the hollow fiber filter, tubing, connectors, and pump heads. While significant attention is typically directed toward the filter module, the remaining components of the hydraulic loop are often neglected. A robust and well-balanced hydraulic loop design must fulfill the following requirements:

1. **Minimize shear stress for the cells:** Hydrodynamic shear stress is generated throughout the cell retention loop, including within tubing and the hollow fiber lumen, at transitions between components, such as abrupt changes in inner diameter without smooth tapering, and within the pump head. Shear stress generated in the centrifugal pump is mainly driven by impeller speed. Therefore, reducing the hydraulic system load can help lower the required pump speeds and, consequently shear exposure. Accurately calculating or experimentally determining shear stress (Equation (9)), especially inside the pump head, is complex and its biological impact varies by cell type and cell line (Neunstoecklin et al. 2015). However, it is widely recognized as good practice to minimize shear throughout the loop to ensure scalability.
2. **Minimize the residence time of cells outside the bioreactor:** Cells circulating through the cell retention loop are temporarily removed from the controlled environment of the bioreactor, where critical process parameters such as temperature, pH, and dissolved oxygen (DO) are tightly regulated. At high cell densities, DO can be depleted within seconds, resulting in hypoxic conditions that may negatively impact cell health and process performance (Lee 2022). Therefore, it is essential to minimize the time cells spend outside the bioreactor. In addition, the hydraulic loop should be designed to eliminate dead zones or regions of low flow velocity, as these can increase the residence time of cells outside the bioreactor.
3. **Minimizing gas bubble intake into the cell retention loop and ensuring efficient removal:** Due to the high level of sparging in most perfusion bioreactors, gas bubbles can intermittently enter the cell retention loop. It is essential to minimize the intake of these bubbles and to efficiently remove any that do enter. Accumulated bubbles can disrupt flow stability, interfere with flow sensor readings and, in particular, may cause de-priming of the centrifugal pump or the entire cell retention loop.

To fulfill these loop design requirements, appropriate qualitative design choices (e.g. material, connector design, positioning of components) and quantitative design choices (e.g. tubing ID and length, connector ID, pump size) must be considered.

3.2.3.1 | *Qualitative Hydraulic Loop Design Considerations*

Qualitative design choices begin with the selection of component materials. A smooth surface finish is preferred to minimize shear stress (Monroe et al. 1981; Maruyama et al. 2006, 2005). Common tubing materials include platinum-cured silicone or weldable thermoplastic elastomers (TPEs) with similar surface characteristics. Biocompatible polypropylene (PP), polysulfone (PS), and polycarbonate (PC) are typically used for connectors, sensors, and pump heads. Stainless steel is an option, particularly in large scale manufacturing. Ideally, the hydraulic loop should remain free of restrictions and maintain a consistent inner diameter throughout the entire cell retention loop, except for the HF filter module and the pump head. This means that connectors should match the inner diameter of the adjacent tubing, including dip tubes used in small-scale bioreactors. Special attention should be paid to avoiding tubing bends, as these can reduce the inner diameter and impair flow characteristics. When connectors have significantly smaller inner diameters, the resulting transitions can cause increased shear stress and increase the overall hydraulic system load, which in turn forces the pump to operate at higher impeller tip speeds. Conversely, sudden expansions in inner diameter can create regions prone to bubble accumulation or cell settling due to reduced fluid flow velocities. In practice, it is not always feasible to maintain identical inner diameters across the entire cell retention loop. In such cases, smooth transitions in reducer connectors should be used to avoid turbulence and minimize shear stress.

Initial priming of the cell retention loop and maintaining a well-primed cell retention loop is crucial to ensure robust perfusion operation. The centrifugal pump should be positioned below the

10970290, 0, Downloaded from https://analyticalsciencejournals.onlinelibrary.wiley.com/doi/10.1002/bit.70335 by Fachhochschule Nordwestschweiz, Wiley Online Library on [28/08/2026]. See the Terms and Conditions (https://onlinelibrary.wiley.com/terms-and-conditions) on Wiley Online Library for rules of use; OA articles are governed by the applicable Creative Commons License

bioreactor liquid level such that the hydrostatic pressure primes the pump initially through the bottom outlet of the bioreactor. Mitigating gas bubble intake is another crucial design consideration. The placement of the outlet (leading into the cell retention device) should ensure that bubbles from the sparger are not directly drawn into the cell retention loop. Given the stirring direction, it is ideal to place the outlet prior to the sparger along the flow path in order to minimize gas bubble intake. When working with dip tubes at bench-top scale, common practice is to extend the dip tube with a silicone tube to a position protected from bubble intake, for example, below the sparger.

Even with optimal design choices, bubbles occasionally enter the cell retention loop. In some cases, these bubbles can cause de-priming of the pump head or even the entire loop. Pump head de-priming is typically a concern only with the smallest centrifugal pump sizes, where the bubble size is significant relative to the pump head volume. In these situations, bubbles can become trapped at the center of the rotating impeller. Although temporarily increasing pump speed to expel trapped bubbles is a feasible solution, this approach also increases flow rates and alters the wall-shear rate within the hollow fiber (HF) module, with unknown consequences for filtration performance. A more widely adopted industry strategy is to orient the pump head outlet at a 45° angle, which ensures that the opening leading to the outlet is positioned at the highest point of the pump head. During periodic pump stops of a few seconds, rising gas bubbles can then exit through this opening, preventing bubble entrapment without affecting the wall shear rate. At larger scales, pumps are less prone to de-priming because the bubble size becomes negligible compared to the pump head volume, allowing bubbles to be flushed out without the need for specific removal strategies. Loop de-priming can be mitigated through quantitative design choices such as selecting appropriate tubing inner diameters.

3.2.3.2 | *Quantitative Hydraulic Loop Design Considerations*

Scale adaptation is required to adjust for the scale-specific fluid flow rate (crossflow), which is defined by the process-specific design choices that were made based on the wall-shear rate target within the HF filter module. Given the fixed fluid flow rate, the main levers to adjust hydraulic system load, residence time, and bubble removal are tube inner diameter and tube length. While both tube ID and length impact the hydraulic system load and increase loop holdup volume, only tube ID influences the fluid velocity. For simplicity in the following hydraulic perspective, it is assumed that connectors have a similar ID to the tubing and tubes and connectors are simply referred to as the loop.

3.2.3.2.1 | *Hydraulic System Load Minimization*

Shear rate arising from high fluid velocities in the loop can be reduced by enlarging the loop inner diameter and estimated using Equation (7). In contrast, shear stress generated within the pump head is significantly more complex to calculate and is beyond the scope of this manuscript. However, a pragmatic approach is to minimize the hydraulic system load, enabling the pump to operate at the lowest possible speed while still meeting residence time and bubble removal requirements. To assess the impact of loop ID or loop length changes on hydraulic system load, the Darcy-Weisbach equation can be applied (Equations (10)–(13)). The overall hydraulic system load of a cell retention setup consists of contributions from the HF filter, the loop (tubing and connectors), and the pump. Each section of the loop can be evaluated individually using the Darcy-Weisbach equation, and the total system load is obtained by summing these contributions (Equation (14)). Ideally, the HF module should dominate the total hydraulic system load, and the contribution from the remaining loop components should be minimized. When a sufficiently large pump is selected, such that the inlet and outlet fittings do not restrict flow, the pump's contribution can generally be neglected. The HF module contribution is fixed, as it is defined by the target wall-shear rate specified in the process design and cannot be adjusted at this stage. In contrast, loop contributions can be reduced either by increasing the loop ID or by shortening the loop length and minimizing bends.

Although minimizing the loop's contribution to the overall hydraulic load is generally desirable, large-scale cell retention systems may still impose higher overall hydraulic loads despite optimization efforts. Contributing factors for overall hydraulic system load include increased HF module length at larger scales, raising its share of the total load, longer tubing runs due to bioreactor positioning constraints, and limited options imposed by fixed bioreactor port dimensions. Maintaining a consistent overall hydraulic system load across scales is considered good practice to ensure similar pump operating conditions and impeller tip speeds across different scales. Accordingly, loop ID and loop length serve as key parameters for tuning hydraulic load and can be adjusted in scale-down models to better emulate large-scale performance. However, design changes that alter system load also affect fluid velocity and loop holdup volume. Therefore, such adjustments must remain within ranges that satisfy residence time requirements and ensure effective bubble removal.

3.2.3.2.2 | *Residence Time Constraint*

Increasing loop inner diameter and tubing length both lead to a higher holdup volume in the cell retention loop. Given that the fluid flow rate is predefined based on the target wall-shear rate in the HF module, any increase in holdup volume will inevitably result in a longer residence time for the cells within the loop. Accurate estimation of residence time requires consideration of the entire holdup volume, including the tubing, pump head, and HF filter volumes (Equation (15)). Oxygen is the limiting substrate when it comes to determining the residence time in the cell retention loop. An oxygen gradient or even depletion cannot be fully prevented due to high metabolic activity of high cell density processes. However, it is worth noting, that cells experience repeated oxygen gradients (or even depletions) in larger scales with mixing times of up to 100 s without reported detrimental impact (Villiger et al. 2018). While no universally critical residence time of cells in the retention loop has been established, residence time should be minimized and most TFF perfusion systems usually operate below 30 to 60 s, below mixing times of many established large scale processes (Walther et al. 2019).

10970290, 0, Downloaded from https://analyticalsciencejournals.onlinelibrary.wiley.com/doi/10.1002/bit.70335 by Fachhochschule Nordwestschweiz, Wiley Online Library on [28/08/2026]. See the Terms and Conditions (https://onlinelibrary.wiley.com/terms-and-conditions) on Wiley Online Library for rules of use; OA articles are governed by the applicable Creative Commons License

3.2.3.2.3 | Bubble Washout Considerations

When the holdup volume of the cell retention loop increases due to a larger loop inner diameter, and the volumetric flow rate remains constant, the resulting linear flow velocity decreases (Equation (6)). While lower flow velocity can reduce shear stress, excessively low velocities compromise efficient washout of gas bubbles from the cell retention loop back to the bioreactor. Bubble accumulation occurs when the buoyant rise velocity exceeds the downward fluid flow velocity. Under such conditions, bubbles are no longer transported effectively, particularly in loop segments with vertical downward flow, where buoyancy opposes the flow direction (Figure 3A). Over time, inefficient bubble removal can lead to gas accumulation and eventual de-priming of the system. While large gas bubbles typically accumulate at the highest point of the loop, often above the HF module, accumulation in horizontal segments is also observed. To overcome the resistance from trapped gas, the centrifugal pump must operate at higher impeller speeds, thereby increasing shear stress. Initially, fluid flow may be sustained, but persistent accumulation can ultimately result in complete de-priming. In a de-priming event, the entire cell retention loop, including the pump head, fills with gas, resulting in a loss of flow and failure of the cell retention device, ultimately leading to termination of the perfusion process. Defining the critical fluid flow velocities below which bubble washout cannot be guaranteed is essential for robust design of cell retention devices. To address this, screening experiments were conducted to estimate critical bubble removal velocities (Figure 3B). As buoyant force and thus terminal rise velocity increase with bubble size according to Archimedes' principle, screening experiments were performed using macro bubbles generated through an injection hole of 2.5 mm to determine the critical flow velocities required to ensure washout of the worst-case bubble sizes. All experiments were performed at 37°C using water–glycerin mixtures of varying viscosities to mimic the rheological properties of cell culture media. The results showed that the critical bubble removal flow velocity depends on both loop inner diameter and fluid viscosity. As loop ID increased from 1/8 inch to 3/4 inch, the critical flow velocity for bubble removal rose sharply from 0.12 to 0.47 m/s. Beyond a loop ID of 3/4 inch, a plateau was observed at approximately 0.55 m/s at a viscosity of 0.7 cP. This trend was corroborated at higher viscosities (2.5 cP and 5.0 cP), representative of high-density perfusion cultures, with viscosity producing a modest decrease in the critical bubble removal velocity across all loop IDs. Terminal bubble rise velocities were determined to be between 20 and 30 cm/s for single bubble of a size between 1 and 10 mm in the literature (Baz-Rodriguez et al. 2012). The lower critical flow velocities observed in smaller tubing sizes (1/8 inch and 1/4 inch) can be attributed to the reduced inner diameters, where the wall proximity restricts the relative motion of the liquid around the bubble, thereby slowing its rise (Uno and Kintner 1956). Furthermore, the higher critical flow velocities observed in larger tubing sizes (1/2 inch and above) may be explained by the hydrodynamic velocity profile within the tube, where liquid velocity is lower near the wall and bubbles migrate across regions with different local velocities. From a practical standpoint, perfusion cultures typically start at low cell densities with fluid viscosities close to that of water at 37°C. Thus, designing the cell retention loop to maintain flow velocities above the 0.7 cP-derived critical threshold provides a conservative safety margin, ensuring reliable bubble removal even as viscosity increases over the perfusion process. Notably, the length of the cell retention loop does not impact bubble removal efficiency, as it does not alter the linear fluid flow velocity.

In summary, the key challenge is to minimize shear stress on the cells while maintaining sufficient flow velocity to ensure acceptable residence time and effective gas bubble removal within the cell retention loop. Achieving this balance requires

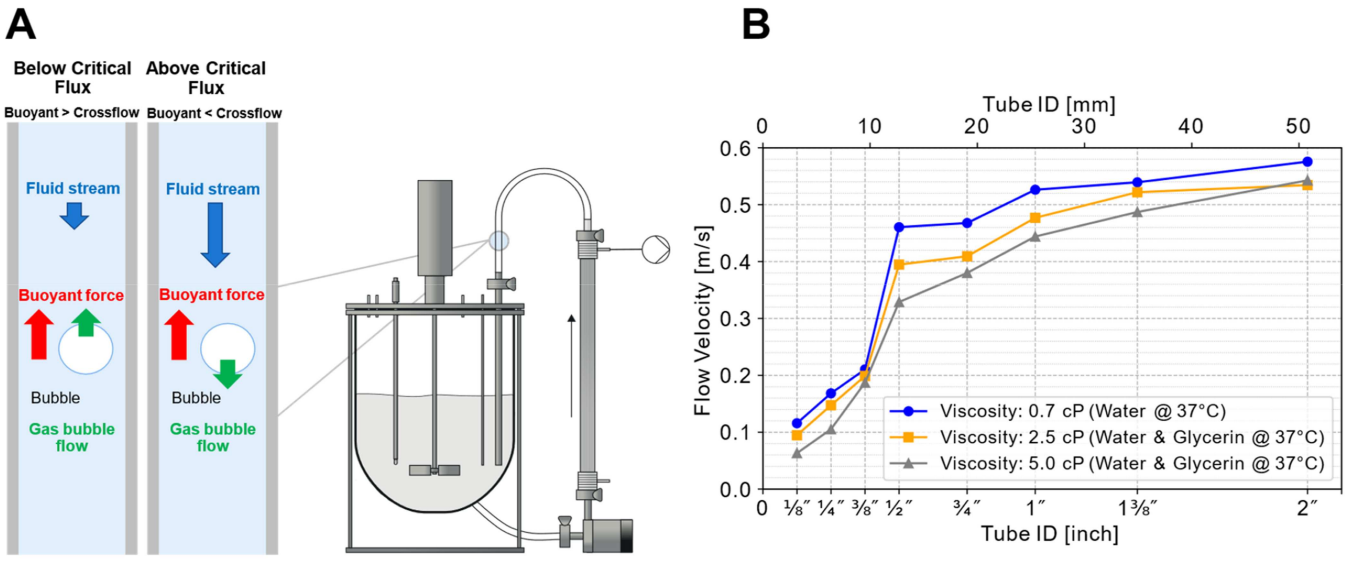

FIGURE 3 | (A) Schematic representation highlighting the opposing effects of the downward fluid stream and the upward buoyant force on gas bubble motion within vertical tubing, leading to bubble accumulation in case of insufficient fluid flow velocity. (B) Critical bubble removal velocity as a function of inner diameter (ID) of silicone tubing, measured at three different fluid viscosities (0.7 cP, 2.5 cP, and 5.0 cP), corresponding perfusion process relevant fluid viscosities.

10970290, 0, Downloaded from https://analyticalsciencejournals.onlinelibrary.wiley.com/doi/10.1002/bit.70335 by Fachhochschule Nordwestschweiz, Wiley Online Library on [28/08/2026]. See the Terms and Conditions (https://onlinelibrary.wiley.com/terms-and-conditions) on Wiley Online Library for rules of use; OA articles are governed by the applicable Creative Commons License

integrating qualitative design considerations with quantitative criteria to trade off shear reduction against residence time and bubble washout constraints.

3.2.4 | *Pump Selection*

In theory, an ideal scale-up strategy would select and operate a pump such that the shear stress exposure generated within the pump head remains constant across scales, thereby promoting a consistent cellular response and minimizing unexpected outcomes during scale-up. In practice, however, accurately calculating or modeling the shear stress within a centrifugal pump head under specific operating conditions is highly complex and requires numerous assumptions. Factors such as the number of culture turnovers per day, the residence time of cells within critical zones, and changing medium composition as well as viscosity during the cell culture process can impact the cellular response to shear exposure. These variables are difficult to precisely quantify and introduce uncertainty that renders precise shear estimation impractical. Considering these challenges, a pragmatic, experimentally driven approach is recommended to guide pump selection and operating conditions for robust, scalable cell retention processes. Namely, to reduce risks associated with scale-up by designing larger-scale systems that are comparable to, or gentler on, cells than their small-scale counterparts. Demonstrating performance under representative or worst-case conditions at small scale provides confidence that centrifugal pump-related parameters are compatible with cell viability and establishes a reliable baseline for scale-up. This strategy prioritizes the importance of maintaining or improving critical process parameters for the pump during scale-up. These include preserving constant impeller tip speed, ensuring equal or reduced culture turnover rates, and maintaining or lowering the residence time per turnover within the pump head. These considerations are essential during scale-up for several key reasons:

i. Pump impeller tip speed (Equation (16)) is a critical process parameter during scale-up. Although absolute recommendations are not provided here, given the substantial variability in shear susceptibility across cell types and cell lines, careful design of the cell retention device to reduce impeller tip speed typically leads to operating conditions under which no adverse effects on the cell culture are observed. On scale-up, impeller tip speeds should not increase beyond those encountered in development experiments. The rotational speed (in rpm) needed to generate sufficient pressure to overcome the hydraulic system load (Figure 4A) varies across pump sizes due to different impeller sizes (SI Table 3). With careful centrifugal pump head design, pumps of different sizes can achieve comparable pressures at similar impeller tip speeds (Figure 4B). Appropriate pump sizing can be determined from pump head-specific pressure-flow characterization curves (Figure 4C–G), which include contour lines that represent constant impeller tip speeds. At low fluid flow rates, these contour lines are typically horizontal, indicating that the pressure required is largely independent of flow rate and that the same impeller tip speed is sufficient to generate the required pressure, and increasing the flow rate does not significantly increase the tip speed. However, as the fluid flow rate rises further, the contour lines begin to dip or slope downward, reflecting the pump's increasing internal hydraulic resistance at higher flow rates. This resistance arises from restrictions within the pump head and its inlet and outlet. In practical terms, further increases in flow rate beyond this point require higher impeller tip speeds, which can elevate shear stress. When operation departs from the near-horizontal contour region, switching to a larger pump head is advisable. Owing to its larger internal flow paths and connections, the higher flow will again fall within the more favorable, near-horizontal region of the pressure-flow curve for the larger pump size, allowing impeller tip speed to remain within acceptable limits. A transition to a larger pump head, however, increases the residence time of cells in the pump head per turnover because of the larger pump head volume (Equation (18)). This trade-off must be carefully balanced against the benefit of lower shear associated with reduced impeller tip speeds. Therefore, selecting the smallest centrifugal pump that operates within the horizontal contour region at the intended flow rate is generally recommended. In certain flow ranges, two pump head sizes may be suitable: a smaller pump running at a somewhat higher impeller tip speed, or a larger pump operating at a lower tip speed but with longer cell residence time per turnover. In such cases, a case-by-case assessment is recommended. Based on these principles, the authors propose suitable flow rate-to-pump size pairings to support pump selection (Figure 4H).

ii. By design, the gap between the impeller and the pump head housing increases with pump size. While estimating shear stress using a simplified model, treating the impeller as a moving wall and the pump housing as a stationary wall, does not capture the full complexity of shear generation within a centrifugal pump, it suggests that a larger gap reduces shear stress (Equation (8)). From this simplified perspective, scale-up by maintaining constant tip speeds inherently reduces shear stress due to the increased impeller-to-housing gap and can be considered a conservative and robust strategy that mitigates the risk of scale-related shear damage.

iii. Under the reasonable assumption that fewer culture turnovers through the pump head are either beneficial or neutral for cell culture performance, the scale-up objective should be to achieve similar or fewer turnovers than at small-scale (Yeleswarapu et al. 1995). When the selected filter permits constant filter length across scales, and both lumen wall-shear rate and the flux are held constant, the ratio of fluid flow to vessel volume remains unchanged, and thus the number of culture turnovers through the centrifugal pump head remains constant (17). If longer filters are used during scale-up while maintaining constant LMH and wall-shear rate within the fiber lumen, the fluid flow increases, but the vessel volume increases even more. This results in a reduced turnover frequency as scale increases. In both scenarios, the number of turnovers remains constant or decreases, which is in favor of the scaling approach.

iv. Another factor preferentially maintained or minimized during scale-up is the residence time that cells spend in

10970290, 0, Downloaded from https://analyticalsciencejournals.onlinelibrary.wiley.com/doi/10.1002/bit.70335 by Fachhochschule Nordwestschweiz, Wiley Online Library on [28/08/2026]. See the Terms and Conditions (https://onlinelibrary.wiley.com/terms-and-conditions) on Wiley Online Library for rules of use; OA articles are governed by the applicable Creative Commons License

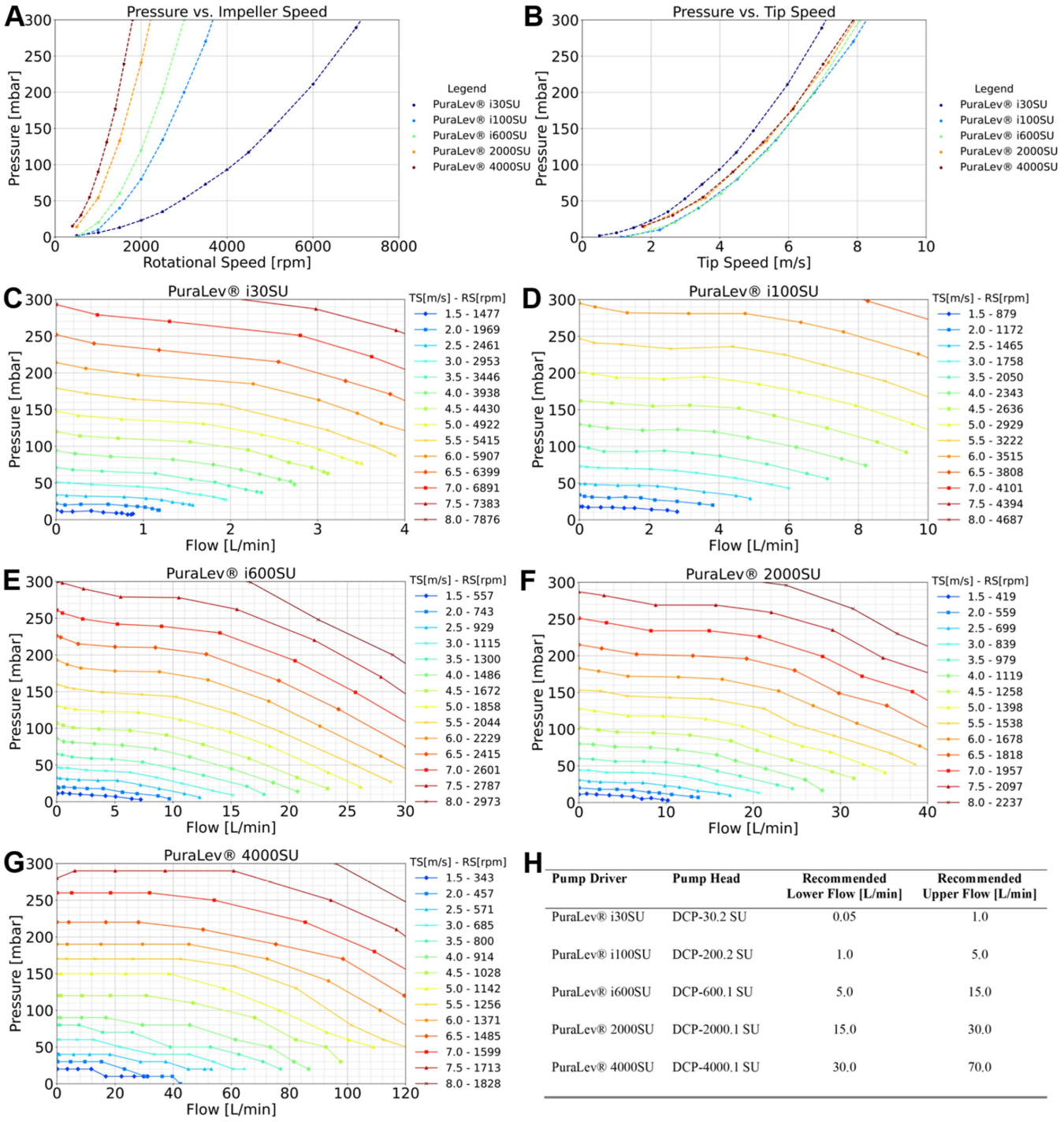

H

Pump Driver	Pump Head	Recommended Lower Flow [L/min]	Recommended Upper Flow [L/min]
PuraLev® i30SU	DCP-30.2 SU	0.05	1.0
PuraLev® i100SU	DCP-200.2 SU	1.0	5.0
PuraLev® i600SU	DCP-600.1 SU	5.0	15.0
PuraLev® 2000SU	DCP-2000.1 SU	15.0	30.0
PuraLev® 4000SU	DCP-4000.1 SU	30.0	70.0

FIGURE 4 | Characterization data of the levitated centrifugal pump line in water at 37°C. Pressure generated by the pump versus rotational speed required for all pump models in horizontal contour range can be found in (A), while rotational speed was converted to impeller tip speed in (B). Pressure-flow curves for pumps are grouped according to pump model: DCP-30.2 (C), DCP-200.2 (D), DCP-600.1 (E), DCP-2000.1 (F), and DCP-4000.1 (G). Contour lines are colored according to tip speed (TS[m/s]), which is unified across pump scales. Plot (H) shows the recommended flow rates for each corresponding pump based on the pump characterization.

the pump head per turnover (Leverett et al. 1972; Ding et al. 2015). This residence time depends on the fluid flow velocity and the pump head volume (18). Maintaining, or preferably reducing pump head residence time at larger scales helps de-risk the scale-up process. Residence time is often longest at small scale, where pump heads may be oversized relative to the required flow rate, leading to prolonged exposure within the pump. At larger scales, a broader range of pump head sizes is available, allowing more precise pump sizing and thereby reducing residence time within the pump head. Although the authors cannot define a specific critical residence time, a practical design principle is to ensure that the maximum residence time occurs at small scale, where targeted screening experiments

10970290, 0, Downloaded from https://analyticalsciencejournals.onlinelibrary.wiley.com/doi/10.1002/bit.70335 by Fachhochschule Nordwestschweiz, Wiley Online Library on [28/08/2026]. See the Terms and Conditions (https://onlinelibrary.wiley.com/terms-and-conditions) on Wiley Online Library for rules of use; OA articles are governed by the applicable Creative Commons License

should be performed to confirm no adverse effect on cell culture performance, thereby providing a pragmatic basis for robust scale-up.

3.3 | Multi-Filter Systems

Beyond a certain bioreactor size, a single filter cell retention device may no longer suffice. At that point, multi-filter configurations will be required to increase filtration surface area to maintain the target LMH. In processes where product sieving is a high priority (e.g. steady-state perfusion), multi-filter setups often become necessary above 500 L perfusion bioreactor volume. By contrast, for strategies where sieving is less critical, such as N-1 perfusion, or for modalities where monoclonal antibodies (mAbs) are retained within the bioreactor, a single filter can remain adequate at volumes of several thousand liters due to the higher LMH targets achievable before necessitating multiple filters. Several different multi-filter setup designs are feasible, each with its own advantages and drawbacks (Figure 5).

3.3.1 | Single-Module Multi-Loop Setup

The simplest way to implement a multi-filter system is to scale out (Figure 5A). This means simply duplicating the cell retention loop using the largest available filter. The primary advantage of scaling out is the ability to replicate the successful small-scale loop design without modifications. This approach ensures a secure scale-up process, especially beneficial when only a few filter modules (e.g., two or three) are needed. By multiplying the entire loop, the system gains redundancy, as each filter operates independently with precise flow control for each module. The scaling-out approach reaches its limitations with a larger number of filters, as each loop requires two bioreactor ports, one for the feed and one for the retentate of the cell retention device which should be positioned to prevent short-circuiting of the culture volume. This approach is often used in steady-state perfusion at around 1000 L to 1500 L, as well as in N-1 perfusion or in processes where mAbs are retained in the bioreactor and a single filtration module is no longer sufficient.

3.3.2 | Parallel Multi-Filter Setup

Parallelizing hollow fiber (HF) filter modules reduces the number of cell retention loops, and thus the number of required bioreactor ports, while still increasing the total filtration area (Figure 5B). This enables very compact filtration skids in which a single pump feeds two or more HF filter modules. From a hydraulic perspective, parallelizing the hollow fiber (HF) filter modules does not increase the hydraulic contribution by the filter, since the crossflow velocity and fiber length remain unchanged. The fluid flow path is usually split by a Y-piece upstream of the HF filter modules and then merged on the retentate side of the loop. As the fluid path is split, per-branch flow rates drop significantly, which has major implications for the tubing design. A clear distinction must be made between “cluster” tubing, which runs from the bioreactor to the Y-split and from the merging Y-piece back to the bioreactor, and “filter” tubing, which connects directly to the HF filter modules and carries fluid at a lower velocity. When applying the scaling principles described in this manuscript, tubing dimensions must be selected independently for cluster and filter tubing to meet their specific flow requirements. This ensures compliance with all critical design criteria, including minimal hydraulic load, sufficiently short residence time in the cell retention loop, and effective bubble washout. The main limitation of parallelization is the increased fluid flow in the cluster tubing, setting higher requirements for the centrifugal

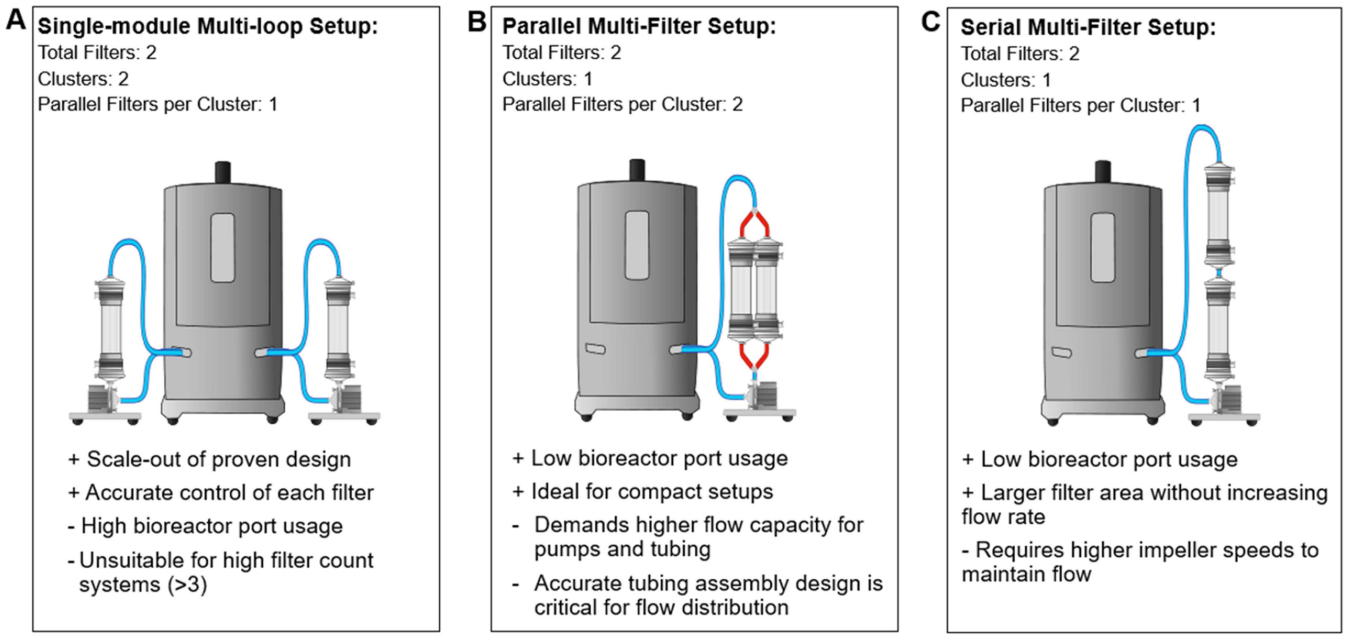

FIGURE 5 | Schematic representation of multi-filter configurations for production-scale bioreactors. The setups include (A) a scale-out approach with two independent systems, each consisting of one filter and one pump, (B) parallel configuration with a single pump distributing cell broth across two filters simultaneously, and (C) serial configuration with a single pump sequentially feeding cell broth through two filters.

10970290, 0, Downloaded from https://analyticalsciencejournals.onlinelibrary.wiley.com/doi/10.1002/bit.70335 by Fachhochschule Nordwestschweiz, Wiley Online Library on [28/08/2026]. See the Terms and Conditions (https://onlinelibrary.wiley.com/terms-and-conditions) on Wiley Online Library for rules of use; OA articles are governed by the applicable Creative Commons License

pump. While two-module parallelization is feasible and widely used in industry, extending to higher degrees of parallelization becomes challenging, particularly in single-use systems, due to constraints on available tubing sizes. A practical compromise is to use a multi-loop parallel setup consisting of multiple independent cell retention loops, each with two parallel HF filter modules (SI Figure 3). The general trend of reducing wall-shear rate within the fiber lumen enables operation at lower crossflows, which in turn reduces the cluster flow rate and makes parallelization of more than two filters more viable. Nevertheless, additional trade-offs include reduced control over exact flow distribution among modules and increased design complexity. Parallel HF filter configurations are most commonly employed in perfusion processes with low LMH requirements, such as steady-state perfusion at bioreactor volumes above 1000 L.

3.3.3 | *Serial Multi-Filter Setup*

While serial multi-filter configurations can also be used to increase filtration area without requiring additional bioreactor ports, they differ fundamentally from the parallelization approach (Figure 5C). First, as HF filter modules are arranged in series, their hydraulic contributions are additive, directly increasing pump power demand and necessitating higher impeller tip speeds to overcome the additional pressure drop. Consequently, serial setups can be challenging when using small-lumen-ID filters, which already impose substantial hydraulic load. In contrast, large-lumen-ID filters with inherently lower hydraulic resistance are more suitable for serial arrangements. Second, despite the added filtration area, the total loop flow rate remains the same as in a single-filter setup. This can be advantageous, as it avoids tubing size limitations and reduces demand on pump size and power. Although serial multi-filter setups are less common in the industry due to the increased hydraulic load and associated rise in impeller tip speed, they can be a viable option when employing large-lumen-ID HF filters operated at reduced wall-shear rates. Overall, parallel, serial, and hybrid multi-filter configurations (SI Figure 3) enable highly compact filtration skids with significant floor space savings. These configurations increase filtration area while requiring fewer bioreactor ports than single-module multi-loop cell retention systems. Additionally, they simplify priming and integrity testing and provide greater flexibility in positioning the cell retention device, making it possible to place the system in a more convenient location rather than directly adjacent to the bioreactor.

3.4 | TFF Perfusion Scaling Strategy Examples

To demonstrate the proposed scaling approach in practice, two example strategies are presented using two widely adopted types of HF modules in the industry. The first HF module line maintains a consistent fiber length across scales, while the second features variable fiber lengths and a larger lumen inner diameter. Together, these two module types capture the diversity of commercially available HF modules and are representative of the broader market. From a process perspective, a steady-state perfusion process, characterized by typical parameters including a cell culture viscosity of 2 cP, perfusion rate of 1.5 vvd, bleed rate of 15%, filtrate flux of approximately 3 $L/m^2/h$, and wall-shear rate of 800 s^{-1} in the HF lumen. The same scaling approach is applicable to N-1 perfusion and other specialized strategies with minor adjustments to the input parameters. A commonly used multi-filter strategy involving two parallel HF modules per cluster was selected, with further scale-up achieved by multiplying these two-module clusters to reach the required filtration area. While other multi-filter strategies are also feasible, this configuration serves as a robust and practical example for demonstrating the scaling approach.

3.4.1 | *Scaling Strategy for Constant Length HF Module*

The scaling strategy for the HF module family with a constant 65 cm fiber length (Table 1) maintains similar Starling flow across scales, supporting process reproducibility. An LMH of approximately 3 $L/m^2/h$ was achieved by slightly adjusting the bioreactor fill volume. Alternatively, recirculation loops at bench scale could be introduced or perfusion could be operated at a higher LMH, depending on the process needs. All cell retention device designs up to and including 500 L were designed as single-filter setups. For 1000 L and above, multi-filter configurations became necessary. Fluid flow rates in the recirculation loop ranged from 66 mL/min at the smallest scale to 31.5 L/min at the 1000 L and 2000 L scales. These flow rates are moderate and compatible with commercially available tubing IDs. The overall hydraulic system load was tuned to approximately 50 to 55 mbar across scales, while maintaining residence time below 25 s and ensuring sufficiently high flow velocities to prevent gas bubble accumulation. Due to the constant filter length, the hydraulic load contribution from the HF filter remained consistent at 42 mbar across all scales. Consequently, loop contributions were likewise minimized and held as constant as practical to sustain a low overall system load. Pump selection based on pressure-flow curve characterization resulted in very similar impeller tip speeds, ranging from 3.1 to 3.9 m/s. The authors consider this range sufficiently consistent, especially given that the gap between the impeller and pump housing increases with pump size, which inherently reduces shear. If desired, further alignment of impeller tip speeds could be achieved by adjusting tubing lengths, although such changes would also impact other critical parameters, including loop residence time. Culture turnover through the cell retention device was maintained across scales, and pump-head residence time per turnover was also consistent, except for the worst-case configuration at the smallest scale. This overall consistency indicates a reliable and predictable scale-up strategy.

3.4.2 | *Scaling Strategy for Variable Length and Larger Lumen Inner Diameter HF Module*

Increasing HF module length with increasing filter size (Table 2) elevates Starling flow, which can adversely impact filtration performance. However, the larger lumen inner diameter (ID) of 1.4 mm, compared with the commonly used 1.0 mm, helps to reduce the pressure drop across the filter, thereby lowering Starling flow. As in the previous example, bioreactor fill volumes were adjusted to achieve the target flux of approximately 3 LMH, using the available HF modules.

10970290, 0, Downloaded from https://analyticalsciencejournals.onlinelibrary.wiley.com/doi/10.1002/bit.70335 by Fachhochschule Nordwestschweiz, Wiley Online Library on [28/08/2026]. See the Terms and Conditions (https://onlinelibrary.wiley.com/terms-and-conditions) on Wiley Online Library for rules of use; OA articles are governed by the applicable Creative Commons License

TABLE 1 | TFF perfusion scaling output for constant length HF modules. Suggested TFF perfusion scaling using a constant length HF module across various perfusion bioreactor scales.

Process information								
Bioreactor Size	2	10	50	200	500	1000	2000	L
Reactor Fill Volume	1.7	8.5	30	150	400	800	1600	L
Perfusion Rate	1.5	1.5	1.5	1.5	1.5	1.5	1.5	vvd
Bleed Rate	15	15	15	15	15	15	15	%
Harvest Rate	2.2	10.8	38.3	191	510	1020	2040	L/day
Culture Viscosity	2	2	2	2	2	2	2	cP
Filter module information								
Filter Manufacturer	Repligen	Repligen	Repligen	Repligen	Repligen	Repligen	Repligen	—
Filter Cat. Number	D06-P20U-10-N	S06-P20U-10-N	N06-P20U-10-N	K06-P20U-10-N	X06-P20U-10-N	X06-P20U-10-N	X06-P20U-10-N	—
Membrane Chemistry	PES	PES	PES	PES	PES	PES	PES	—
Membrane Pore Size	0.2	0.2	0.2	0.2	0.2	0.2	0.2	μm
HF Length	0.65	0.65	0.65	0.65	0.65	0.65	0.65	m
Lumen ID	1	1	1	1	1	1	1	mm
Membrane Area per HF Module	0.03	0.15	0.51	2.55	7.15	7.15	7.15	7.15
Target Wall-shear Rate	800	800	800	800	800	800	800	1/s
Filtrate Flux (LMH)	3.11	3.01	3.13	3.13	2.97	2.97	2.97	$L/m^2/h$
Single/Multi-filter Architecture								
Total # of HF Modules	1	1	1	1	1	2	4	—
Total # of Clusters/Pumps	1	1	1	1	1	1	2	—
# Parallel Filter per Cluster	1	1	1	1	1	2	2	—
HF Membrane Area per Cluster	0.03	0.15	0.51	2.55	7.15	14.30	14.30	m^2
Total HF Membrane Area	0.03	0.15	0.51	2.55	7.15	14.30	28.60	m^2
Cluster Tubing Flow Rate	66	353	1178	5890	15787	31573	31573	mL/min
Filter Tubing Flow Rate	66	353	1178	5890	15787	15787	15787	mL/min
Residence Time in Loop per Turnover	25	22	24	17	21	19	19	s
Tubing Selection								
Cluster Tubing ID	1/8	1/4	3/8	5/8	1	1 1/4	1 1/4	inch
Cluster Tubing Length	1.5	2.5	3	3	6	5	5	m
Cluster Tubing Flow Velocity	0.14	0.19	0.28	0.50	0.52	0.66	0.66	m/s
Filter Tubing ID	—	—	—	—	—	1	1	inch
Filter Tubing Length	—	—	—	—	—	1	1	m
Filter Tubing Flow Velocity	—	—	—	—	—	0.52	0.52	m/s

(Continues)

10970290, 0, Downloaded from https://analyticalsciencejournals.onlinelibrary.wiley.com/doi/10.1002/bit.70335 by Fachhochschule Nordwestschweiz, Wiley Online Library on [28/08/2026]. See the Terms and Conditions (https://onlinelibrary.wiley.com/terms-and-conditions) on Wiley Online Library for rules of use; OA articles are governed by the applicable Creative Commons License

TABLE 1 | (Continued)

Hydraulic System Load								
HF Module Hydraulic Contribution	42	42	42	42	42	42	42	mbar
Cluster Tubing Hydraulic Contribution	13	7	6	10	11	11	11	mbar
Filter Tubing Hydraulic Contribution	—	—	—	—	—	2	2	mbar
Overall Hydraulic System Load	55	49	47	51	53	54	54	mbar
Pump Selection								
PuraLev® Pump Motor	i30SU	i30SU	i100SU	i600SU	i2000SU	4000SU	4000SU	—
PuraLev® Pump Head (DCP)	30.2SU	30.2SU	200.2SU	600.1SU	2000.1SU	4000.1SU	4000.1SU	—
Turnovers through Pump	56	60	57	57	57	57	57	1/day
Residence Time in Pump per Turnover	7.0	1.3	1.2	1.2	1.0	1.3	1.3	s
Rotational Pump Speed	3100	3000	1600	1450	1100	800	800	rpm
Impeller Tip Speed	3.1	3.0	3.6	3.9	3.9	3.5	3.5	m/s

Single-filter cell retention setups were feasible up to the 500 L bioreactor scale. Because of the larger lumen ID, higher loop flow rates, ranging from 272 mL/min to 55.6 L/min, were required to reach the target wall-shear rate of 800 s^{-1}. This, in turn, necessitates larger tubing IDs across all scales relative to the constant-length, 1.0 mm lumen ID example. Despite the higher flow rates, residence time per turnover in the loop remained below 20 s across all scales. As the HF module length increased with scale, its hydraulic load contribution rose from 10 mbar at the smallest scale to 43 mbar at the largest. This increase was balanced by designing the loop to contribute more to the hydraulic load at small scales and progressively less at larger scales, resulting in similar overall system loads of approximately 50 to 60 mbar. Pump impeller tip speeds remained between 3.3 and 3.9 m/s, except at 200 L and 500 L scales, where slightly higher tip speeds of 4.4 and 4.8 m/s were observed. These elevated tip speeds reflect operation on the downward-sloping region of the pressure-flow curve, suggesting that the next-larger pump size may be preferable. Switching up a size, as shown in brackets in Table 2, would reduce tip speed to 3.6 m/s at both scales. However, this change would also increase the pump-head residence time per turnover by nearly threefold. Which option is superior for culture performance, or whether both perform equally well, must be determined case-by-case. This example further highlights the complexity of balancing interdependent process parameters and the importance of understanding the impact of design changes. Notably, the number of culture turnovers decreases sharply from 340 at the smallest scale to 80 at the largest. The high turnover rate at small scale is driven by the lower HF module length at that scale. Provided that small-scale studies demonstrate no adverse impact on culture performance, the declining turnover frequency with scale is a favorable indicator of robust scale-up.

4 | Conclusion

This manuscript addresses the challenge of translating successful small-scale TFF perfusion processes to manufacturing scale by proposing a structured, data-driven framework. A four-step workflow, comprising process scaling, filter scaling, hydraulic loop design and pump selection, was developed. This workflow offers a practical and effective strategy for designing robust TFF perfusion systems, despite the inherent complexity of the process. Grounded in established industry practices and augmented by detailed hydraulic and pump characterization data, the approach enables users to move beyond empirical, trial-and-error methods toward more predictable and scalable designs. The workflow can be applied to common hollow fiber modules, including multi-filter setups at large scale. Importantly, the methodology is broadly applicable across perfusion modes, including steady-state perfusion, dynamic perfusion, N-1 perfusion, perfused batch, and processes in which the product is retained by the HF filter, and extends to emerging modalities such as cell and gene therapies. By bridging the gap between small-scale success and large-scale implementation, this framework supports the development of reliable, high-performance perfusion systems and representative scale-down models for the biopharmaceutical industry.

10970290, 0, Downloaded from https://analyticalsciencejournals.onlinelibrary.wiley.com/doi/10.1002/bit.70335 by Fachhochschule Nordwestschweiz, Wiley Online Library on [28/08/2026]. See the Terms and Conditions (https://onlinelibrary.wiley.com/terms-and-conditions) on Wiley Online Library for rules of use; OA articles are governed by the applicable Creative Commons License

TABLE 2 | TFF perfusion scaling output for variable length HF modules. Suggested TFF perfusion scaling using a variable length HF module across various perfusion bioreactor scales.

Process information								
Bioreactor Size	2	10	50	200	500	1000	2000	L
Reactor Fill Volume	1.15	5	45	200	500	1000	2000	L
Perfusion Rate	1.5	1.5	1.5	1.5	1.5	1.5	1.5	vvd
Bleed Rate	15	15	15	15	15	15	15	%
Harvest Rate	1.5	6.4	57.4	255	637	1275	2550	L/day
Culture Viscosity	2	2	2	2	2	2	2	cP
Filter module information								
Filter Manufacturer	Asahi	Asahi	Asahi	Asahi	Asahi	Asahi	Asahi	—
Filter Cat. Number	UMP-0047R	UMP-1047R	UMP-2147R	UMP-3247R	UMP-5247R	UMP-5247R	UMP-5247R	—
Membrane Chemistry	PVDF	PVDF	PVDF	PVDF	PVDF	PVDF	PVDF	—
Membrane Pore Size	0.2	0.2	0.2	0.2	0.2	0.2	0.2	μm
HF Length	0.21	0.21	0.43	1	0.94	0.94	0.94	m
Lumen ID	1.4	1.4	1.4	1.4	1.4	1.4	1.4	mm
Membrane Area per HF Module	0.02	0.09	0.77	3.8	8.8	8.8	8.8	8.8
Target Wall-shear Rate	800	800	800	800	800	800	800	1/s
Filtrate Flux (LMH)	3.05	2.95	3.10	2.80	3.02	3.02	3.02	$L/m^2/h$
Single/Multi-filter Architecture								
Total # of HF Modules	1	1	1	1	1	2	4	—
Total # of Clusters/Pumps	1	1	1	1	1	1	2	—
# Parallel Filter per Cluster	1	1	1	1	1	2	2	—
HF Membrane Area per Cluster	0.02	0.09	0.77	3.8	8.8	17.6	17.6	m^2
Total HF Membrane Area	0.02	0.09	0.77	3.8	8.8	17.6	35.2	m^2
Cluster Tubing Flow Rate	272	1293	5172	10991	27801	55602	55602	mL/min
Filter Tubing Flow Rate	272	1293	5172	10991	27801	27801	27801	mL/min
Residence Time in Loop per Turnover	6	7	11	16/(16)	19/(20)	16	16	s
Tubing Selection								
Cluster Tubing ID	1/8	1/4	1/2	3/4	1 1/4	1 1/2	1 1/2	inch
Cluster Tubing Length	1.5	3	4	4	6	5	5	m
Cluster Tubing Flow Velocity	0.57	0.68	0.68	0.64	0.59	0.81	0.81	m/s
Filter Tubing ID	—	—	—	—	—	1 1/4	1 1/4	inch
Filter Tubing Length	—	—	—	—	—	1	1	m
Filter Tubing Flow Velocity	—	—	—	—	—	0.59	0.59	m/s

(Continues)

10970290, 0, Downloaded from https://analyticalsciencejournals.onlinelibrary.wiley.com/doi/10.1002/bit.70335 by Fachhochschule Nordwestschweiz, Wiley Online Library on [28/08/2026]. See the Terms and Conditions (https://onlinelibrary.wiley.com/terms-and-conditions) on Wiley Online Library for rules of use; OA articles are governed by the applicable Creative Commons License

TABLE 2 | (Continued)

Hydraulic System Load									
HF Module Hydraulic Contribution	10	10	20	46	43	43	43	43	mbar
Cluster Tubing Hydraulic Contribution	54	32	29	16	10	12	12	12	mbar
Filter Tubing Hydraulic Contribution	—	—	—	—	—	2	2	2	mbar
Overall Hydraulic System Load	64	42	49	61	53	57	57	57	mbar
Pump selection									
PuraLev Pump Motor	i30SU	i100SU	i600SU	i600SU/(2000SU)	i2000SU/(4000SU)	4000SU	4000SU	4000SU	—
PuraLev Pump Head (DCP)	30.1SU	200.2SU	600.1SU	600.1SU/(2000.1SU)	2000.1SU/(4000.1SU)	4000.1SU	4000.1SU	4000.1SU	—
Turnovers through Pump	340	372	166	79	80	80	80	80	1/day
Residence Time in Pump per Turnover	1.7	1.1	1.3	0.6/(1.5)	0.6/(1.5)	0.8	0.8	0.8	s
Rotational Pump Speed	3300	1550	1400	1650/(1000)	1350/(825)	900	900	900	rpm
Impeller Tip Speed	3.3	3.5	3.8	4.4/(3.6)	4.8/(3.6)	3.9	3.9	3.9	m/s

Author Contributions

Patrick Romann: conceptualization, formal analysis, investigation, methodology, visualization, writing – original draft, project administration. **Antony Sibilia:** conceptualization, formal analysis, visualization, project administration. **Philip Giller:** data curation, formal analysis, investigation, methodology, visualization. **Thomas K. Villiger:** conceptualization, methodology, investigation, writing – original draft. **All other authors:** conceptualization, methodology, investigation, writing – review and editing.

Acknowledgments

The authors gratefully acknowledge all contributors who are not specifically named for the many valuable discussions related to this topic, with special thanks to Jürgen Hahn, Stefano Trossarello, Petrit Loshi, Fabian Frank, Ilan Goldberg, Jannis Bähler, Alex Schmid, Philipp Campos, Lorenz Schüssler, and Knut Kuss. Open access publishing facilitated by Fachhochschule Nordwestschweiz FHNW, as part of the Wiley - Fachhochschule Nordwestschweiz FHNW agreement via the Consortium Of Swiss Academic Libraries.

Conflicts of Interest

Patrick Romann, Antony Sibilia, and Philip Giller are employees of Levitronix GmbH, a company that manufactures and markets centrifugal pumps and flow sensors used in this study. This relationship is disclosed in the interest of transparency, however, the authors declare that this has not influenced the design, execution, or interpretation of the work. All authors declare that they have no other competing financial interests or personal relationships that could have appeared to influence the work reported in this paper.

Data Availability Statement

The data that support the findings of this study are available from the corresponding author upon reasonable request.

References

Amer, M., A. Vaca, and M. Bowden. 2022. "Evaluating Shear in Perfusion Rotary Lobe Pump Using Nanoparticle Aggregates and Computational Fluid Dynamics." *Bioprocess and Biosystems Engineering* 45, no. 9: 1477–1488. https://doi.org/10.1007/s00449-022-02757-1.

Baz-Rodriguez, S., A. Aguilar-Corona, and A. Soria. 2012. "'Rising Velocity for Single Bubbles in Pure Liquids." *Revista Mexicana de Ingeniería Química* 11, no. 2: 269–278. http://www.redalyc.org/articulo.oa?id=62026895006.

Bielser, J. M., M. Wolf, J. Souquet, H. Broly, and M. Morbidelli. 2018. *Perfusion Mammalian Cell Culture for Recombinant Protein Manufacturing – A Critical Review*. Elsevier Inc. https://doi.org/10.1016/j.biotechadv.2018.04.011.

Caso, S., M. Aeby, M. Jordan, R. Guillot, and J. M. Bielser. 2022. "Effects of Pyruvate on Primary Metabolism and Product Quality for a High-Density Perfusion Process." *Biotechnology and Bioengineering* 119, no. 4: 1053–1061. https://doi.org/10.1002/bit.28033.

Clincke, M.-F., C. Mölleryd, Y. Zhang, E. Lindskog, K. Walsh, and V. Chotteau. 2011. "Study of a Recombinant Cho Cell Line Producing a Monoclonal Antibody by ATF or TFF External Filter Perfusion in a Wave Bioreactor™." *BMC Protocol* 5, no. S8: P105. https://doi.org/10.1186/1753-6561-5-s8-p105.

Clincke, M. F., C. Mölleryd, Y. Zhang, E. Lindskog, K. Walsh, and V. Chotteau. 2013. "Very High Density of CHO Cells in Perfusion by ATF or TFF in Wave Bioreactor™: Part I: Effect of the Cell Density on the Process'." *Biotechnol. Prog.* 29, no. 3: 754–767. https://doi.org/10.1002/btpr.1704.

10970290, 0, Downloaded from https://analyticalsciencejournals.onlinelibrary.wiley.com/doi/10.1002/bit.70335 by Fachhochschule Nordwestschweiz, Wiley Online Library on [28/08/2026]. See the Terms and Conditions (https://onlinelibrary.wiley.com/terms-and-conditions) on Wiley Online Library for rules of use; OA articles are governed by the applicable Creative Commons License

Coffman, J., M. Brower, L. Connell-Crowley, et al. 2021. "A Common Framework for Integrated and Continuous Biomanufacturing." *Biotechnology Bioengineering* 118, no. 4: 1721–1735. https://doi.org/10.1002/bit.27690.

Ding, J., S. Niu, Z. Chen, T. Zhang, B. P. Griffith, and Z. J. Wu. 2015. "Shear-Induced Hemolysis: Species Differences." *Artificial Organs* 39, no. 9: 795–802. https://doi.org/10.1111/aor.12459.

Fisher, A. C., M.-H. Kamga, C. Agarabi, K. Brorson, S. L. Lee, and S. Yoon. 2019. "The Current Scientific and Regulatory Landscape in Advancing Integrated Continuous Biopharmaceutical Manufacturing." *Trends in Biotechnology* 37, no. 3: 253–267. https://doi.org/10.1016/j.tibtech.2018.08.008.

Johnstone, P., E. Mast, E. Hughes, and H. Peng. 2020. "Development of a Small-Scale Rotary Lobe-Pump Cell Culture Model for Examining Cell Damage in Large-Scale N-1 Seed Perfusion Process." *Biotechnol. Prog.* 36, no. 6: e3044. https://doi.org/10.1002/btpr.3044.

Karst, D. J., E. Serra, T. K. Villiger, M. Soos, and M. Morbidelli. 2016. "Characterization and Comparison of ATF and TFF in Stirred Bioreactors for Continuous Mammalian Cell Culture Processes." *Biochemical Engineering Journal* 110: 17–26. https://doi.org/10.1016/j.bej.2016.02.003.

Kudugunti, K., 'Alternating Tangential Flow Rapid Harvesting', US 2022/0325708 A1, 2022.

Lee, K. 2022. Accessed: Jan. 24, 2026. "Design Considerations When Scaling From 3-L to 3000-L or Larger." *in Integrated Continuous Biomanufacturing V, ECI Symposium Series*, https://dc.engconfintl.org/biomanufact_v/74.

Leverett, L. B., J. D. Hellums, C. P. Alfrey, and E. C. Lynch. 1972. "Red Blood Cell Damage by Shear Stress." *Biophysical Journal* 12, no. 3: 257–273. https://doi.org/10.1016/S0006-3495(72)86085-5.

MacDonald, M. A., M. Nöbel, D. Roche Recinos, et al. 2022. "Perfusion Culture of Chinese Hamster Ovary Cells for Bioprocessing Applications." *Taylor and Francis Ltd* 42, no. 7: 1099–1115. https://doi.org/10.1080/07388551.2021.1998821.

Madabhushi, S. R., Q. Zuo, C. Zhou, et al. 2025. "Systematic Investigation of Impact of Antifoam and Extracellular Vesicles on Fouling of Hollow Fiber Filters in Intensified Perfusion Processes Highlights the Key Impact of Antifoam." *Biotechnology and Bioengineering* 122, no. 7: 1684–1695. https://doi.org/10.1002/bit.28987.

Maruyama, O., Y. Numata, M. Nishida, et al. 2005. "Hemolysis Caused by Surface Roughness under Shear Flow." *Journal of Artificial Organs* 8, no. 4: 228–236. https://doi.org/10.1007/s10047-005-0316-x.

Maruyama, O., M. Nishida, T. Yamane, I. Oshima, Y. Adachi, and T. Masuzawa. 2006. "Hemolysis Resulting From Surface Roughness Under Shear Flow Conditions Using a Rotational Shear Stressor." *Artificial Organs* 30, no. 5: 365–370. https://doi.org/10.1111/j.1525-1594.2006.00227.x.

Matanguihan, C., and P. Wu. 2022. "Upstream Continuous Processing: Recent Advances in Production of Biopharmaceuticals and Challenges in Manufacturing." *Current Opinion in Biotechnology* 78: 102828. https://doi.org/10.1016/j.copbio.2022.102828.

Merivirta, M., Improvement of Quality Control of extruded Tubes With online Optical Measuring Techniques, 2017.

Metze, S., S. Ruhl, G. Greller, C. Grimm, and J. Scholz. 2020. "Monitoring Online Biomass With a Capacitance Sensor During Scale-Up of Industrially Relevant CHO Cell Culture Fed-Batch Processes in Single-Use Bioreactors." *Bioprocess and Biosystems Engineering* 43, no. 2: 193–205. https://doi.org/10.1007/s00449-019-02216-4.

Monroe, J. M., D. E. True, and M. C. Williams. 1981. "Surface Roughness and Edge Geometries in Hemolysis With Rotating Disk Flow." *Journal of Biomedical Materials Research* 15, no. 6: 923–939. https://doi.org/10.1002/jbm.820150616.

Neunstoecklin, B., M. Stettler, T. Solacroup, H. Broly, M. Morbidelli, and M. Soos. 2015. "Determination of the Maximum Operating Range of Hydrodynamic Stress in Mammalian Cell Culture." *Journal of Biotechnology* 194: 100–109, Jan. https://doi.org/10.1016/j.jbiotec.2014.12.003.

Pappenreiter, M., H. Schwarz, B. Sissolak, and A. Jungbauer. 2023. "Product Sieving of Mab and Its High Molecular Weight Species in Different Modes of ATF and TFF Perfusion Cell Cultures." *Journal of Chemical Technology & Biotechnology* 98, no. 7: 1658–1672. https://doi.org/10.1002/jctb.7386.

Pavlik, R., 'United States Patent', US 2019/0201820 A1, 2019a.

Pavlik, R., 'Australian Patent', WO 2019/133487 A1, 2019b.

Pinto, N. D. S., and M. Brower. 2020. "Wide-Surface Pore Microfiltration Membrane Drastically Improves Sieving Decay in TFF-Based Perfusion Cell Culture and Streamline Chromatography Integration for Continuous Bioprocessing." *Biotechnology and Bioengineering* 117, no. 11: 3336–3344, Nov. https://doi.org/10.1002/bit.27504.

Radoniqi, F., H. Zhang, C. L. Bardliving, P. Shamlou, and J. Coffman. 2018. "Computational Fluid Dynamic Modeling of Alternating Tangential Flow Filtration for Perfusion Cell Culture." *Biotechnology and Bioengineering* 115, no. 11: 2751–2759. https://doi.org/10.1002/bit.26813.

Raza, H., T. Tang, B. Gao, C. Phuangthong, C. B. Chen, and N. D. S. Pinto. 2024. "Evaluation of Various Membranes at Different Fluxes to Enable Large-Volume Single-Use Perfusion Bioreactors." *Biotechnology and Bioengineering* 121, no. 9: 2678–2690. https://doi.org/10.1002/bit.28722.

Recanati, G., M. Pappenreiter, C. Gstoettner, et al. 2023. "Integration of a Perfusion Reactor and Continuous Precipitation in An Entirely Membrane-Based Process for Antibody Capture." *Engineering in Life Sciences* 23, no. 10: e2300219. https://doi.org/10.1002/elsc.202300219.

van Reis, R., S. Gadam, L. N. Frautschy, et al. 1997. "High Performance Tangential Flow Filtration." *Biotechnology and Bioengineering* 56, no. 1: 71–82. https://doi.org/10.1002/(SICI)1097-0290(19971005)56:1<71::AID-BIT8>3.0.CO;2-S.

Reynolds, O., 'An Experimental Investigation of the Circumstances Which Determine Whether the Motion of Water Shall Be Direct or Sinuous, and of the Law of Resistance in Parallel Channels', 1883. Accessed: Jan. 24, 2026. [Online]. http://www.jstor.org/stable/109431.

Romann, P., P. Giller, A. Sibilia, et al. 2024. "Co-Current Filtrate Flow in TFF Perfusion Processes: Decoupling Transmembrane Pressure From Crossflow to Improve Product Sieving." *Biotechnology and Bioengineering* 121, no. 2: 640–654. https://doi.org/10.1002/bit.28589.

Romann, P., J. Kolar, L. Chappuis, C. Herwig, T. K. Villiger, and J. M. Bielser. 2023. "Maximizing Yield of Perfusion Cell Culture Processes: Evaluation and Scale-Up of Continuous Bleed Recycling." *Biochemical Engineering Journal* 193: 108873. https://doi.org/10.1016/j.bej.2023.108873.

Schaub, J., A. Ankenbauer, T. Habicher, et al. 2024. "Process Intensification in Biopharmaceutical Process Development and Production – An Industrial Perspective." *Walter de Gruyter GmbH* 9, no. 9: 2989–3041. https://doi.org/10.1515/psr-2022-0113.

Shevitz, J., 'United States Patent', US 2018/0236407 A1, 2018.

Sibilia, A., 'Device and a Method for Tangential Flow Filtration of a Fluid', US20220395770A1, 2022.

Starling, E. H. 1896. "on the Absorption of Fluids From the Connective Tissue Spaces." *The Journal of Physiology* 19, no. 4: 312–326. https://doi.org/10.1113/jphysiol.1896.sp000596.

Stepper, L., F. A. Filser, S. Fischer, J. Schaub, I. Gorr, and R. Voges. 2020. "Pre-Stage Perfusion and Ultra-High Seeding Cell Density in Cho Fed-Batch Culture: A Case Study for Process Intensification Guided by Systems Biotechnology." *Bioprocess and Biosystems Engineering* 43, no. 8: 1431–1443. https://doi.org/10.1007/s00449-020-02337-1.

10970290, 0, Downloaded from https://analyticalsciencejournals.onlinelibrary.wiley.com/doi/10.1002/bit.70335 by Fachhochschule Nordwestschweiz, Wiley Online Library on [28/08/2026]. See the Terms and Conditions (https://onlinelibrary.wiley.com/terms-and-conditions) on Wiley Online Library for rules of use; OA articles are governed by the applicable Creative Commons License

Tregidgo, M., M. Dorn, C. Lucas, and M. Micheletti. 2023. "Design and Characterization of a Novel Perfusion Reactor for Biopharmaceuticals Production." *Chemical Engineering Research and Design* 194: 344–357. https://doi.org/10.1016/j.cherd.2023.04.066.

Uno, S., and R. C. Kintner. 1956. "Effect of Wall Proximity on the Rate of Rise of Single Air Bubbles in a Quiescent Liquid." *AIChE Journal* 2, no. 3: 420–425. https://doi.org/10.1002/aic.690020323.

Veje, M. H., M. Quirós, P. Kristensen, and M. K. Jørgensen. 2024. "Investigation of Fouling in Perfusion Cell Culture Processes Using Alternating Tangential Flow Filtration." *Journal of Membrane Science* 701: 122764. https://doi.org/10.1016/j.memsci.2024.122764.

Villiger, T. K., B. Neunstoecklin, D. J. Karst, et al. 2018. "Experimental and Cfd Physical Characterization of Animal Cell Bioreactors: From Micro- to Production Scale." *Biochemical Engineering Journal* 131: 84–94. https://doi.org/10.1016/j.bej.2017.12.004.

Vu, J., J. A. Gadberry, J. Coffman, and K. Lee. 2024. "Improved Sieving Coefficient in Perfusion Cell Culture With Reduced Effective Filtration Length of Hollow Fibers." *Biotechnology Progress* 40, no. 5: e3472. https://doi.org/10.1002/btpr.3472.

Walther, J., J. McLarty, and T. Johnson. 2019. "The Effects of Alternating Tangential Flow (Atf) Residence Time, Hydrodynamic Stress, and Filtration Flux on High-Density Perfusion Cell Culture." *Biotechnology and Bioengineering* 116, no. 2: 320–332. https://doi.org/10.1002/bit.26811.

Wang, S., S. Godfrey, J. Ravikrishnan, H. Lin, J. Vogel, and J. Coffman. 2017. "Shear Contributions to Cell Culture Performance and Product Recovery in ATF and TFF Perfusion Systems." *Journal of Biotechnology* 246: 52–60. https://doi.org/10.1016/j.jbiotec.2017.01.020.

Weinberger, M. E., L. Schoch, and U. Kulozik. 2023. "New Technical Concept for Alternating Tangential Flow Filtration in Biotechnological Cell Separation Processes." *Biotechnology Progress* 39, no. 2: e3309. https://doi.org/10.1002/btpr.3309.

Wolf, M., J.-M. Bielser, and M. Morbidell. 2020. *Perfusion Cell Culture Processes for Biopharmaceuticals: Process Development, Design, and Scale-up*. Cambridge University Press.

WuDunn, D., A. Squeri, J. Vu, A. Dhingra, J. Coffman, and K. Lee. 2024. "Effect of Inner Diameter, Filter Length, and Pore Size on Hollow Fiber Filter Fouling During Perfusion Cell Culture." *Biotechnology Progress* 40, no. 3: e3440. https://doi.org/10.1002/btpr.3440.

Yeleswarapu, K. K., J. F. Antaki, M. V. Kameneva, and K. R. Rajagopal. 1995. "A Mathematical Model for Shear-Induced Hemolysis." *Artificial Organs* 19, no. 7: 576–582, Jul. https://doi.org/10.1111/j.1525-1594.1995.tb02384.x.

Zamani, L., M. Lundqvist, Y. Zhang, et al. 2018. "High Cell Density Perfusion Culture Has a Maintained Exoproteome and Metabolome." *Biotechnology Journal* 13, no. 10: 01800036. https://doi.org/10.1002/biot.201800036.

Supporting Information

Additional supporting information can be found online in the Supporting Information section.
Supporting File: bit70335-sup-0001-2026_04_20_TFF_Supporting_Information.docx.

10970290, 0, Downloaded from https://analyticalsciencejournals.onlinelibrary.wiley.com/doi/10.1002/bit.70335 by Fachhochschule Nordwestschweiz, Wiley Online Library on [28/08/2026]. See the Terms and Conditions (https://onlinelibrary.wiley.com/terms-and-conditions) on Wiley Online Library for rules of use; OA articles are governed by the applicable Creative Commons License